Cellular-Assisted Vehicular Communications: A Stochastic Geometric Approach

Sayantan Guha

Thesis submitted to the Faculty of the

Virginia Polytechnic Institute and State University

in partial fulfillment of the requirements for the degree of

Master of Science

in

Electrical Engineering

Harpreet S. Dhillon, Co-Chair

Carl B. Dietrich, Co-Chair

J. Michael Ruohoniemi

Oct 15,2015

Blacksburg, Virginia

Cellular Assisted Vehicular Communications: A Stochastic Geometric Approach

Sayantan Guha

ABSTRACT

A major component of future communication systems is vehicle-to-vehicle (V2V) communications, in which vehicles along roadways transfer information directly among themselves and with roadside infrastructure. Despite its numerous potential advantages, V2V communication suffers from one inherent shortcoming: the stochastic and time-varying nature of the node distributions in a vehicular ad hoc network (VANET) often leads to loss of connectivity and lower coverage. One possible way to improve this coverage is to allow the vehicular nodes to connect to the more reliable cellular network, especially in cases of loss of connectivity in the vehicular network. In this thesis, we analyze this possibility of boosting performance of VANETs, especially their node coverage, by taking assistance from the cellular network.

The spatial locations of the vehicular nodes in a VANET exhibit a unique characteristic: they always lie on roadways, which are predominantly *linear* but are irregularly placed on a two dimensional plane. While there has been a significant work on modeling wireless networks using random spatial models, most of it uses homogeneous planar Poisson Point Process (PPP) to maintain tractability, which is clearly not applicable to VANETs. Therefore, to accurately capture the spatial distribution of vehicles in a VANET, we model the roads using the so called Poisson Line Process and then place vehicles randomly on each road according to a one-dimensional homogeneous PPP. As is usually the case, the locations of the cellular base stations are modeled by a planar two-dimensional PPP. Therefore, in this thesis, we propose a new *two-tier* model for cellular-assisted VANETs, where the cellular base stations form a planar PPP and the vehicular nodes form a one-dimensional PPP on roads modeled as undirected lines according to a Poisson Line Process.

The key contribution of this thesis is the stochastic geometric analysis of a maximum power-based cellular-assisted VANET scheme, in which a vehicle receives information from either the nearest vehicle or the nearest cellular base station, based on the received power. We have characterized the network interference and obtained expressions for coverage probability in this cellular-assisted VANET, and successfully demonstrated that using this switching technique can provide a significant improvement in coverage and thus provide better vehicular network performance in the future. In addition, this thesis also analyzes two threshold-distance

based schemes which trade off network coverage for a reduction in additional cellular network load; notably, these schemes also outperform traditional vehicular networks that do not use any cellular assistance. Thus, this thesis mathematically validates the possibility of improving VANET performance using cellular networks.

Acknowledgement

I would like to take this opportunity to thank my thesis advisor Dr Harpreet Singh Dhillon, for the enormous support, guidance and encouragement that he has provided me over the last one year. It was his immense technical knowledge, ideas and constant feedback that has made this thesis possible. Working under him has been a pleasure and I am extremely thankful to him for providing me with the opportunity to be a part of his research group.

I also want to express my heartfelt thanks and gratitude to Dr Carl B Dietrich, who advised me through most of my MS, helped me understand the world of vehicular communications and provided me with the financial support that made possible my completion of this Master's degree and the writing of this thesis.

I am also grateful to Dr John Michael Ruohoniemi for agreeing to be on my committee, as well as for his excellent teaching of "Radio Wave Propagation" and "Radar Systems Design", both of which gave me a deep technical understanding of these areas, and of wireless communications in general.

My parents have been a constant source of love and encouragement through almost every important task of my life, and writing this thesis was no different. I am extremely thankful for the sacrifices they have made for me, and the numerous ways in which they have been a guiding light of inspiration.

Contents

List of Figures

List of Notations

Symbol	Meaning
o	Origin (Location of Receiver)
μ	Density of Vehicles
λ	Density of Roads
(r, θ)	Polar Coordinates of Projection o on a line
λ_a	Density of Cellular MBSs
$\frac{1}{\epsilon_v}$	Transmit Power of vehicle
$\frac{1}{\epsilon_M}$	Transmit Power of cellular MBS
N_v	Number of Vehicles
N_{roads}	Number of Roads
d_{th}	Threshold Distance
α	Path Loss Coefficient
T	Threshold SIR (Signal-to-Interference Ratio)
ρ	Distance from o to transmitter being connected to
d_v	Distance from o to nearest vehicle
d_M	Distance from o to nearest cellular MBS
Φ_v	Network of Vehicles on other roads
Φ_r	Network of Vehicles on the same road as o
Φ_M	Network of Cellular MBSs
r_v	Minimum Possible Distance to an interfering vehicle on another road

r_r Minimum Possible Distance to an interfering vehicle on the same road as o

r_M Minimum Possible Distance to an interfering MBS

I_Φ Interference originating from a network Φ

$\mathcal{L}_I$ Laplace transform of Interference

$\mathbb{P}_v$ Probability of connecting to nearest vehicle

$\mathbb{P}_{MBS}$ Probability of connecting to nearest MBS

$\mathbb{P}_{cov|v}$ Probability of Coverage when connecting to a Vehicle

$\mathbb{P}_{cov|MBS}$ Probability of Coverage when connecting to an MBS

$\mathbb{P}_{cov}$ Probability of Coverage

Chapter 1

Introduction

Vehicular ad hoc networks (VANETs) are an area of vital importance in modern wireless communications research, especially because of their growing importance in the development of Intelligent Transportation Systems (ITS). Vehicle-to-vehicle (V2V) communication is being used for a wide variety of purposes such as infotainment, dissemination of traffic data and, most importantly, road safety [1]. For example, V2V communication can be used to avoid rear-end collisions on highways [2], thus potentially saving thousands of lives every year in the United States and across the world. It can also help improve driver comfort by assisting parking based on the availability of nearby parking slots, providing live food and lodging information and even streaming videos for the entertainment of passengers [3].

The most common set of protocols used for V2V communications is DSRC (Dedicated Short Range Communications) [4], which essentially uses direct, line-of-sight communications amongst vehicles and with roadside infrastructure in order to propagate messages throughout a network. For example, an approaching train at a railroad crossing can broadcast a short warning message to all neighboring vehicles, thus preventing possibly fatal train-to-vehicle collisions. Because of its low latency, DSRC has enormous applicability in such safety messaging applications. Also, a DSRC channel has a bandwidth of 10 MHz [5] unlike other short-range communication protocols such as Wi-Fi (which has a much higher bandwidth of 20 MHz). This lower bandwidth provides relatively better robustness to fast fading, thus making DSRC a suitable protocol for dealing with the high mobility of nodes in vehicular networks.

1.1 Motivation

Despite its numerous advantages, the DSRC-based messaging schemes often suffer from one inherent disadvantage: since vehicles are randomly distributed along the roadways, it is often times a realistic possibility that a particular vehicular node does not have any other vehicular nodes in its vicinity and is thus is unable to receive data from any other vehicles in the network. In order to ensure connectivity even in such situations, it is often suggested that Road-Side Units (RSUs) be deployed uniformly along roadways. These RSUs act as relays and broadcast data to all vehicles inside their transmission range, thus providing a better connectivity to the vehicles on the road. However, deployment, installation and maintenance of such a large number of RSUs on every roadway, can be extremely costly and often impractical.

Motivated by this, this thesis looks at a more realistic solution in which the VANET takes support from the cellular network (either without deploying RSUs at all or by deploying them very sparsely) in case of loss of VANET connectivity. In particular, we focus on the spatial modeling of such a network with the eventual goal of drawing system design guidelines. Due to the random and irregular nature of VANETs, stochastic geometry [6] and point process theory [7] provides a natural toolset for their modeling analysis. Therefore, in this thesis, we develop a novel stochastic geometric model of a vehicular network, which is then analyzed to study network performance metrics such as interference distribution, inter-node distances and coverage probability in cellular-assisted VANETs. Before providing more details, we summarize the prior art next.

1.2 Background and Prior Art

1.2.1 V2V Communication

Vehicular communication is a cornerstone of current research on automobile technologies, as well as on wireless networking. A wide range of potential applications, as well as possible PHY and MAC layer protocols, have been put forward for both V2V and V2I (Vehicle-to-Infrastructure) communications. While V2I is taking place using existing wireless technologies such as WiFi, Bluetooth and Infrared [8], DSRC (Dedicated Short Range Communications) is the most common set of protocols for V2V communications. As stated above, DSRC refers to direct, line-of-sight communication among vehicles, taking place in a licensed 75MHz

of spectrum allocated in the 5.9 GHz band [9]. Due to its low latency, robustness to fading and absence of spectrum fees, DSRC is expected to be the primary mode of V2V communications in the future [10].

DSRC can be used for a wide range of applications: infotainment, dissemination of traffic information, parking etc. For example, [11] develops an algorithm that predicts highway travel time based on data collected using DSRC. In [12], the authors propose a DSRC-based V2I communication system, in which Road-Side Units can inform vehicles about the location of empty parking spots, thus reducing street parking times by a large degree. That being said, the biggest potential applicability of V2V communications is in road safety. This includes slow vehicle warnings, lane change warnings, intersection collision warning and cooperative cruise control [13], to name a few. In most of these safety applications, a warning message is generated in case of an event, such as a collision, and is disseminated among the nearby vehicles [13].

1.2.2 Stochastic Geometry for Wireless Networks

Wireless networks often contain nodes that are irregularly and randomly deployed in space. A recent example from mainstream communications areas is that of heterogeneous cellular networks [14; 15], where several types of low power base stations called *small cells* are often deployed at the areas of high user activity, thus resulting in a fairly irregular deployment of base stations across space. This irregularity is not captured very well with the conventional deterministic models, such as the classical hexagonal grid model often used for the macro base station locations [16]. This has led to an increasing interest in the area of applied probability, called stochastic geometry, which allows to capture the irregularity and randomness in the locations of wireless nodes by modeling them as random point processes (basically random spatial patterns) [6; 17]. The added randomness also lends tractability to the models, which usually results in easy-to-use expressions for the key performance metrics of interest, which was not quite possible with the conventional deterministic models.

Stochastic geometry has traditionally been applied more to the analysis of ad hoc networks, e.g., see [18; 19]. The general idea is to model the locations of the transmitters as a homogeneous Poisson Point Process (PPP) on $\mathbb{R}^2$ with the receiver corresponding to each transmitter located uniformly at random on a disk of a fixed radius around that transmitter. More recently, these tools have also become relevant for cellular networks, especially due to the transition to the heterogeneity and capacity-driven deployments of small

cells [20; 21; 22; 23]. A usual direction here is to model the locations of both the base stations and the users as independent PPPs and perform downlink analysis at a typical user (chosen at random from the user point process). Unlike ad hoc networks, where this pairing is done *a priori*, serving base station for a typical user in a cellular network is chosen based on a predefined rule: usually based on the average received signal strength [21; 24]. On the same lines, the uplink analysis of cellular networks has also been performed using these tools [25]. Other applications of stochastic geometry in wireless communications include the modeling and analysis of device-to-device networks [26; 27], cognitive radio networks [28; 29], energy-efficient sensor networks [30], and so on. Since the main goal of this discussion is to provide a general idea of this area, we refer the interested readers to the following authoritative references for a more detailed account of the literature where these tools have been used in the past: [6; 31; 32; 33; 34].

It is worth noting that most of the works in stochastic geometry based analyses in wireless networks have been confined to homogeneous planar PPP-based models to maintain tractability. However, a homogeneous planar PPP is not a reasonable model for vehicular networks. This is because in a planar PPP, the nodes are assumed to be distributed on the plane independently and uniformly. While this is in general true for cellular and some ad hoc networks, it is not true for vehicular networks, where the spatial locations of the wireless nodes (vehicles) exhibit a unique characteristic: they always lie on roadways, which are predominantly *linear* but are irregularly placed on a two dimensional plane. Therefore, a more reasonable probabilistic model should first capture the structure of roadways and then place the nodes randomly on each road. To achieve this, in this thesis, we model roadways as a network of undirected lines according to a Poisson Line Process, and then place vehicles on each road according to a one-dimensional PPP. As is usually the case, the locations of the cellular base stations are modeled by a planar two-dimensional PPP. This leads to a novel *two-tier* setup, which will be used to analyze the performance of cellular-assisted VANETs in this thesis. Before going into further details of the contribution, we provide a brief summary of the stochastic geometry-based analyses of vehicular networks, along with the relevant prior art on Poisson Line Process.

1.2.3   Stochastic Geometry for Vehicular Networks: Poisson Line Process

As noted above, owing to its tractability, homogeneous planar PPP model is usually the primary choice for modeling wireless networks and VANETs are no different. For instance, this model is used in [35] to analyze the performance of broadcast protocols in vehicular communications, and in [36] to study the connection lifetimes between a vehicle and an access point in non-safety VANET applications. In addition, [37] uses a one-dimensional PPP to model the vehicles on a single road and evaluate V2V performance.

However, as discussed earlier in this Chapter, vehicular networks exhibit unique spatial characteristics due to the fact that vehicles can only lie on roadways, which are predominantly *linear* in nature. As a result, a more accurate model for VANETs would be the one which first models the roadways accurately and then places vehicles on each road. One way to achieve this is by modeling the roadways as a network of lines that are distributed on the plane according to a Poisson Line Process (PLP). While PLP will be more formally introduced in Chapter 2, the main idea can be understood as follows. To define a PLP, each line in $\mathbb{R}^2$ is parametrized in terms of its distance and angle from the origin. These distances and angles span a half-cylinder of unit radius. In other words, a point from this unit radius half-cylinder will correspond to a line in $\mathbb{R}^2$. Now, we define a PPP on this half-cylinder and the resulting process of lines formed in $\mathbb{R}^2$ is said to be a PLP. For more details, we refer the reader to the following authoritative references: [7; 17; 38; 39].

Although PLP makes more sense for modeling vehicular networks, the prior art in this direction is surprisingly thin. In [40], the downlink of a cellular network was analyzed in terms of coverage probability by placing vehicular receivers on the lines of a PLP. From the V2V side, [41] uses the PLP model to analyze a VANET and study the rate of multi-hop propagation of messages across the network. It is worth noting that the PLP has also been used for modeling of systems other than vehicular networks. For example, [42] uses PLPs in conjunction with Steiner trees to calculate short-length routes in low-cost networks. It studies, among other things, the mean distance between two fixed points in a PLP, and the perimeter of cells containing both points. Building on these works, we propose a more realistic two-tier model for cellular-assisted VANETs, where the cellular base stations are modeled by a planar PPP and the vehicular nodes are placed on lines modeled according to a PLP. More details about the contributions are provided next.

1.3 Contributions

The main contributions in this thesis are summarized below.

1. *Two-tier model for cellular-assisted VANETs.* This thesis proposes a novel and accurate two-tier model for cellular-assisted VANETs, where the locations of the cellular base stations are modeled by a planar homogeneous PPP, the roadways are modeled according to a Poisson Line Process, and the vehicular nodes are placed on each line (road) of the PLP according to a one-dimensional PPP. This model captures the key characteristic of VANETs: vehicles are located on roadways, which are predominantly linear. This characteristic cannot be accurately captured by using more popular homogeneous PPP-based models. The details of this model are presented in Chapter 2.

2. *Cellular-assisted VANET schemes.* In a cellular-assisted VANET, vehicular nodes can receive information of interest either directly from the nearby vehicles or from the cellular network. Therefore, we have to define schemes that will decide when to connect to a given network. In this thesis, we define and thoroughly analyze the following three schemes:

   (a) *Maximum power based scheme:* In this scheme, the receiving vehicle connects to the tier providing the higher average received power. While this scheme provides the best coverage, it also increases load on the cellular networks by associating most of the vehicles with the cellular base stations.

   (b) *Threshold distance based scheme (inter-road)*: In this scheme, a vehicle connects to its nearest base station only if there exist no vehicular nodes within some predefined threshold distance d_{th} from it. This limits the additional cellular network traffic being generated by the VANET.

   (c) *Threshold Distance Based Scheme (Inter-Road)*: Finally, we study a scheme that limits VANET messaging to take place only within the same road, i.e. if there is no vehicle on the same road as the receiver within a threshold distance, the receiver connects to the nearest cellular base station. In this manner, the VANET traffic is reduced by preventing unncessary transfer of messages amongst different roads in the network.

3. *Coverage analysis.* In Chapters 3 and 4, we analyze the performance of a cellular-assisted VANET using the proposed two-tier model described above. Using tools from stochastic geometry, we derive

analytical expressions for several network parameters such as nearest neighbor distances, tier association probabilities, network interference, and most importantly, probability of coverage at a typical node in the VANET. The analysis is performed for all three cellular-assistance schemes described above.

4. *Key insights and design guidelines.* Chapter 5 presents simulation results for the proposed model, which both validate the analytical results and provide additional design guidelines. Results for both coverage probability and association probabilities to different tiers are provided. These results concretely demonstrate that the cellular network assistance can significantly improve VANET coverage in a variety of scenarios. Several key insights crucial for the design of future cellular-assisted VANETs, such as the choice of the threshold distance in threshold-based schemes, are also provided.

Chapter 2

Network Model

In this thesis, a vehicular ad hoc network is modeled as an urban network of roads with vehicles located along each road in the network. The network of roads is modeled as a Poisson Line Process with intensity λ, with the vehicular nodes along each road having a 1D Poisson distribution of intensity μ. In addition to the direct communication between vehicles, we also consider the possibility of cellular-assisted vehicular communication in which the required information is transmitted to the vehicles by the cellular base stations, which are modeled as a 2D PPP with intensity λ_a. The system model is illustrated in Figure 2.1. In this chapter, we introduce these point processes in the context of the proposed system model.

2.1   Distribution of Vehicular Nodes

As discussed in the next section, all the roads in our proposed model will be modeled as straight lines. The vehicles on each such line are located according to a 1D PPP having an intensity μ. The value of the intensity μ includes that of both vehicles and RSUs, e.g. if both vehicles and RSUs are distributed according to independent PPP's of intensities μ_v and μ_R, the resulting distribution is still a PPP with intensity $\mu = \mu_v + \mu_R$. While we could, in theory, model the locations of the vehicles using other point processes, PPP is usually a natural choice due to its tractability. It is characterized by two properties: (i) the number of points in two disjoint sets is independent, and (ii) the number of points in a 1D PPP with intensity μ that lie within an interval $[a, b]$ is a Poisson random variable of mean $\mu(b - a)$. In other words,
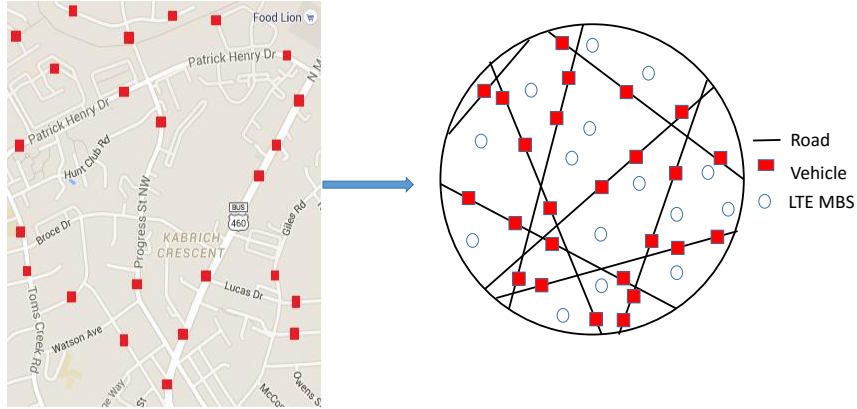
Figure 2.1: *(left)* An illustration of vehicles on actual roads (image courtesy of Google Maps). *(right)* Proposed stochastic geometry-based model for the same network.

for an 1D PPP the probability that there are n points inside an interval of length l is:

$$P[N(l) = n] = \frac{e^{-\mu l}(\mu l)^n}{n!}. \tag{2.1}$$

This definition is easily extendible to higher dimensional Euclidean spaces. See, e.g. [6] for details.

2.2 Distribution of Roads: Poisson Line Process

Due to the predominantly linear nature of the roads, we model them using a Poisson Line Process (PLP) in $\mathbb{R}^2$, which can be thought of as a Poisson Poisson Processes, where instead of points, the undirected lines are randomly distributed on plane [17]. As discussed next, formal description of a PLP involves a parametrization step, in which each line is parameterized in terms of the polar coordinates (r, θ) of the projection of origin o on that line, where $r \in \mathbb{R}, \theta \in [0, 2\pi]$ [17]. Now one can endow points (r, θ) with a distribution, which will endow the lines in $\mathbb{R}^2$ with a distribution. This is discussed next in detail.

2.2.1 Correspondence with a Poisson Point Process

Let D be a line in $\mathbb{R}^2$. As discussed above, let the orthogonal projection of the origin o on this line have the polar coordinates (r, θ), where $r \in \mathbb{R}$ and $\theta \in [0, 2\pi]$ (see Figure 2.2). This transformation of a line D to a point (r, θ) is termed as *parametrization* of the line. Similarly, we can define an application d that uniquely
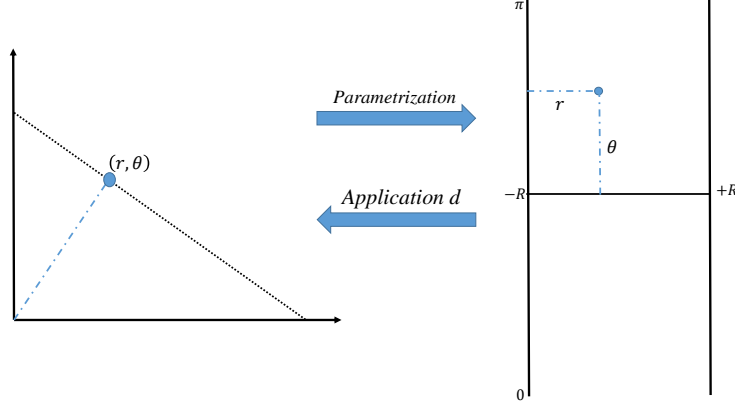
Figure 2.2: Parametrization of a line in terms of (r, θ).

maps a duplet (r, θ) to its corresponding line D (again, see Figure 2.2). Now (r, θ) can be interpreted as

a *point* in a half-cylinder $\mathbb{C}$ of unit radius, defined as $\mathbb{C} = [0, \pi] \times \mathbb{R}$. To endow the lines in $\mathbb{R}^2$ with a

distribution, it is sufficient to endow points in $\mathbb{C}$ with an appropriate distribution. Again, due to tractability,

we assume that the points in $\mathbb{C}$ are modeled by a PPP ζ with the same density λ. The corresponding process

of lines on $\mathbb{R}^2$ is a PLP with density λ. Clearly, as Figure 2.3 shows, for each line in the PLP Φ, there lies a

corresponding point in the PPP ξ, and vice versa. We now study some important properties of PLP next.

2.2.2 Number of Lines inside a Disk in a PLP

Consider a PLP Φ in $\mathbb{R}^2$ as defined above. In this subsection, we shall analyze the number of lines of this

PLP that lie inside a disk B of radius R. Note that for all these lines, $r \in [-R, +R]$ and $\theta \in (0, \pi)$. Thus, the

corresponding points in the PPP ζ lie on a half-cylinder $\mathbb{C} = [0, \pi] \times [-R, +R]$, having a surface area of $\pi \times 2R$.

Hence the expected number of points from the PPP that lie in $\mathbb{C}$ is given by $\mathbb{E}[N_{\text{points}}(\mathbb{C})] = \lambda |\mathbb{C}| = \lambda 2\pi R$.

Since the lines in Φ have a one-to-one correspondence to the points in ζ, the expected number of points

of the corresponding PLP that lie inside the disk is thus also $\mathbb{E}[N_{\text{lines}}(B)] = \lambda 2\pi R$. In other words, for a

Poisson Line Process, *the number of lines lying inside a disk of radius R is a Poisson random variable, with*

a mean that is equal by the product of the intensity λ and the circumference of the disk.

Since in a PPP, conditional on the number of points in any given set, the points are independent and

uniformly distributed in that set, this directly implies that if we condition the number of points of ζ lying
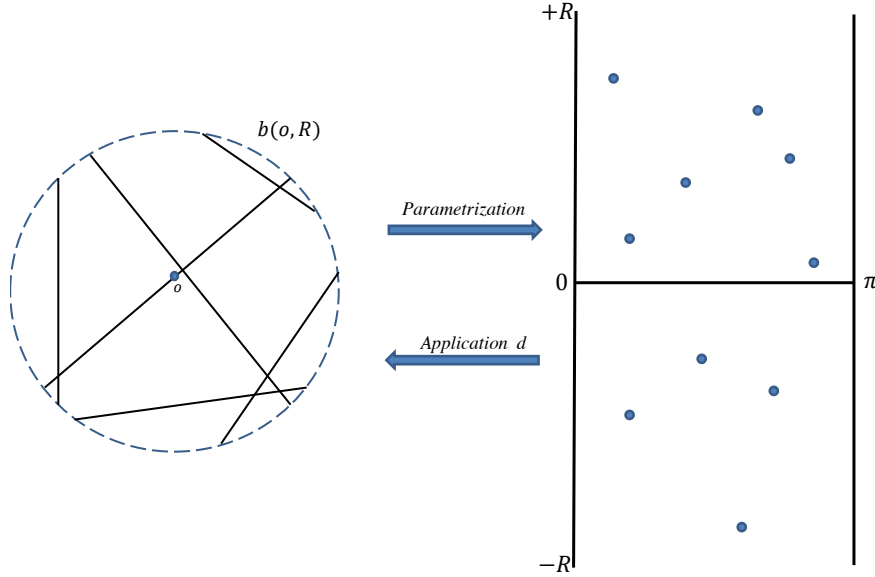
Figure 2.3: Correspondence between PPP and PLP.

in any subset of $\mathbb{C}$, they will be independent and uniformly distributed in that subset. In other words, the r and θ values for each line will follow a uniform distribution over an appropriate range defined by the subset over which the conditioning was done. In the technical arguments, we will be interested in the lines that intersect a ball of given radius or in some cases an annular region of a given inner and outer radius. It is easy to argue using basic properties of a PPP that the number of lines lying between two disks of radius R_1 and R_2 (where $R_2 > R_1$) is a Poisson random variable with intensity $2\pi\lambda(R_2 - R_1)$.

For notational simplicity, the number of roads inside the disk $b(o, R)$ centered at o and having a radius R has been denoted as $N_{roads}(R)$ in the remaining sections of this thesis. Also note that for a road at a distance r from the origin, the segment lying inside the disk has a length of $2\sqrt{R^2 - r^2}$.

Due to the stationarity of the model, our focus will be on the analysis of a vehicle assumed to be located at the origin o. Since all the vehicles are located on some road in the network, then there must always be one road in the PLP that passes through o; i.e. there must be one road with $r = 0$ (we denote this road as D_0). Also, since the PLP is rotation-invariant, we can also assume that D_0 has an angle $\theta = 0$. So, the corresponding PPP always has one point lying on the origin $(0,0)$ of the (r, θ). Therefore, by Slivnyak's theorem, we assert that the remaining roads in the network can be regarded as a PLP itself (i.e. $\Phi \backslash \{D_0\}$ is a PLP) which is independent of D_0. Thus, the network model used in this paper has two independent

11

networks: a PLP with intensity λ ($\Phi \backslash \{D_0\}$) and an additional line (D_0) for which $(r, \theta) = (0, 0)$. Also, by construction the distribution of nodes along different roads are independent of each other.

2.2.3 Null Probability

The null probability for the proposed model is the probability of there being no points (vehicles) inside the disk $b(o, R)$. Many of the mathematical analyses in this thesis, such as association probabilities and CDFs of distance to transmitter, make use of the expression for this null probability; so, we shall now derive it to form the basis for those later analyses. The proof follows directly from the basic properties of a PPP.

Lemma 1. *Null Probability: For a Poisson Line Process Φ with line intensity λ and point intensity μ on each line, the probability that no points exist inside a disk $b(o, R)$ is given by:*

$$\mathbb{P}\left[N(b(o,R)) = 0\right] = 1 - \exp\left[-2\pi\lambda \int_{r=0}^{R} e^{-2\mu\sqrt{R^2-r^2}}\mathrm{d}r\right]. \tag{2.2}$$

Proof. The probability of there being no points of a PLP that lie inside a disk of radius R can be calculated by conditioning over the number of lines n inside the disk, finding the probability of there being no nodes on any of these lines, and then deconditioning over all possible values of n. Thus,

$$\mathbb{P}[N(b(o,R)) = 0] \stackrel{(a)}{=} \sum_{n=0}^{\infty} \mathbb{P}[N_{\mathrm{roads}}(b(o,R)) = n] \times \prod_{i=1}^{n} \mathbb{P}[N_v(\mathrm{road}_i) = 0]$$

$$\stackrel{(b)}{=} \sum_{n=0}^{\infty} \frac{e^{-2\pi\lambda R}(2\pi\lambda R)^n}{n!} \left[\int_{r=-R}^{+R} e^{-2\mu\sqrt{R^2-r^2}}\frac{1}{2R}\mathrm{d}r\right]^n$$

$$\stackrel{(c)}{=} e^{-2\pi\lambda R} \sum_{n=0}^{\infty} \frac{(\pi\lambda \int_{r=-R}^{R} e^{-2\mu\sqrt{R^2-r^2}}\mathrm{d}r)^{\mathrm{n}}}{n!}$$

$$\stackrel{(d)}{=} e^{-2\pi\lambda R} \exp\left[2\pi\lambda \int_{r=0}^{R} e^{-2\mu\sqrt{R^2-r^2}}\mathrm{d}r\right]$$

$$\stackrel{(e)}{=} \exp\left[-2\pi\lambda \int_{r=0}^{R} 1 - e^{-2\mu\sqrt{R^2-r^2}}\mathrm{d}r\right], \tag{2.3}$$

where (a) refers to the fact that if there are n lines in the region $b(o, R)$, then the event of no points occurring in this region is equivalent to that of there being zero points on the segment of each of the n roads inside the disk; the total probability of this event can be calculated by conditioning over the number of roads n, and then deconditioning over all possible values. Step (b) follows from the fact that the number of roads N_{roads}

intersecting $b(o, R)$ is a Poisson random variable with mean $2\pi\lambda R$ (see Subsection 2.2.2), and the number of points in a line segment of length $2\sqrt{R^2 - r^2}$ is a Poisson variable with mean $2\mu\sqrt{R^2 - r^2}$; also r is uniformly distributed from $[-R, +R]$ and independent for each road. Step (d) follows from the property of integral of even functions and from the Taylor series expansion $e^x = \sum_{n=0}^{\infty} \frac{x^n}{n!}$. Finally, step (e) simply makes use of the property that $\int_{R=0}^{\infty} \mathrm{dr} = \mathrm{R}$. This completes the proof. $\hfill\square$

2.3 Cellular Network

Traditionally, cellular networks have been modeled by regularly spaced Macro Base Stations (MBSs), each serving a certain number of Mobile Users inside a regular hexagonal region called a *cell*. However, in recent times, there has been a rapid and irregular deployment of smaller base stations, such as micro-, pico- and femto-cells in order to serve a very rapid increase in number of cellular users and required network throughput. This irregular deployment of Base Stations has made the traditional deterministic model of hexagonal cells quite obsolete, and newer, more probabilistic models with foundations in point processes and stochastic geometry are becoming more realistic [20]. To maintain tractability, the base station locations are usually modeled using 2D homogeneous PPPs [16; 14; 20; 43; 22]. Due to these reasons, this thesis also uses a PPP to model the locations of the cellular Base Stations. For the ease of exposition, we consider only a single type of cellular Base Stations (say, Macro Base Stations) in the thesis. The results can be easily extended to a multi-tier setup, where VANETs may be assisted by a multi-tier cellular network.

Thus, the network model consists of a Poisson line network of roads, interspersed with an independent Poisson network of cellular MBSs. This is thus a two-tier network, the two tiers being the cellular network and the VANET. All the nodes in the same tier have the same transmit power: the MBSs each transmit at a power of $\frac{1}{\epsilon_M}$, while every vehicle has a transmit power of $\frac{1}{\epsilon_v}$. Also, the node distributions in the two tiers are independent of each other. Any receiving node in the network has the option of connecting to either of the tiers based on some selection criteria. The major goal of this thesis is to study the interaction between the two tiers, and to formulate an appropriate set of tier selection criteria that would lead to better network performance, especially in terms of coverage probability at a typical vehicle in the network.

2.4 Safety Messaging

In this thesis, we examine the transfer of safety messages between two nodes in a vehicular ad hoc network. In traditional VANETs, a safety message is triggered in the case of an event; this message is then transmitted to neighboring vehicles and RSUs in the network. Here, we look at schemes in which this message is present not only in the VANET nodes but also in the cellular MBSs; these MBSs can now send these messages to the VANET nodes using the cellular downlink. Thus, a vehicular node can choose to receive its copy of a safety message from either the nearest vehicle or from the nearest MBS, based on some predefined selection criteria. While this would usually lead to an improvement in network performance, this performance gain is highly dependent on the network selection criteria being used. The following section describes three possible cellular-assisted VANET schemes, each with its own set of selection criteria, advantages and disadvantages.

2.5 Cellular-Assisted VANET schemes

As has already been mentioned in Chapter 1, the major focus of this thesis to analyze the network under some schemes by which a VANET receiver can improve coverage by receiving safety messages from the surrounding cellular network, rather than the nodes in the vehicular network, in case of loss of VANET connectivity. This is similar to [21], where a mobile receiver connects to the cellular MBS tier that provides the highest power, as well as the cell selection models discussed in [20; 24] where a cellular UE selects the best cell based on average power . In this thesis, a receiver uses some criteria to connect to one of two tiers: the VANET and the cellular network. Three such selection criteria are discussed:

2.5.1 Maximum Power Based Scheme

In this scheme, the receiver connects to the transmitter (a vehicle or an MBS) from which it receives the highest average power. The receiver selects the nearest vehicle and MBS, and chooses to receive data from the one which supplies a higher time-averaged power. In order to find the received power, we need to first describe the channel model from the transmitters to the receivers, which is done next.

Channel Model: In this thesis, we model both long and short time-scale channel effects. Long time-scale effects are captured by incorporating a distance-based standard power law pathloss with exponent $\alpha > 2$. The short time-scale effects are captured by incorporating channel fading, which is assumed to be Rayleigh distributed. Therefore, if the transmitter transmits at a power of $\frac{1}{\epsilon}$ and is at a distance of ρ from the receiver, the instantaneous power received is given by $P_{rec} = \frac{1}{\epsilon} h \rho^{-\alpha}$, where $h \sim \exp(1)$ models Rayleigh fading and $\rho^{-\alpha}$ is the standard power law pathloss term. Since in practice, it is not preferable to switch from one transmitter to another on the basis of this rapidly varying instantaneous power; so, a time-average of the received power is instead used as the metric for choosing the transmitter. If this averaging time interval is sufficiently higher than the coherence time of the channel, then the average received power is independent of the fading coefficient h, and is given by $P_{av} = \frac{1}{\epsilon} \rho^{-\alpha}$. All nodes in the same tier are assumed to transmit at the same power: every vehicle transmits at $\frac{1}{\epsilon_v}$, while every cellular MBS has a transmit power of $\frac{1}{\epsilon_M}$.

2.5.2 Threshold Distance Based Scheme: Inter-Road

In this scheme, the receiving node takes assistance from the cellular network only when there is no other vehicular node in its vicinity. In other words, the receiver connects to the nearest vehicle when there is at least one vehicle present within a predefined threshold distance d_{th} from it (irrespective of MBS locations), and connects to the nearest MBS when no vehicles are present in this region.

Note that in the two aforementioned schemes, no distinction is made between nodes that are on the same road as the receiver, and those that are on the other roads in the network. The receiver connects to the node supplying the highest power, irrespective of its type or location. As a result, a message generated on one road can get disseminated to other roads in the network as well, especially near intersections (where a vehicle on another road can be closer than all vehicles on the same road). While this is a more generalized model, safety messages in general are relevant to only the nodes on the same road as the transmitting vehicle. For example, if a crash occurs on Highway A, then it is needless to transfer that information to the vehicles on a Highway B that passes Highway A overhead. So, allowing communication across roads can often lead to excessive and unnecessary network loads in the VANET. This motivates us to define another scheme (discussed next), where the communication is confined to the same road.

2.5.3 Threshold Distance Based Scheme: Intra-Road

One way to limit inter-road message communication (and reduce network load), is to allow a node to connect to only those vehicles or RSUs which are on the same road as itself. In order to ensure this, we slightly modify the threshold-distance based scheme discussed above, and allow the receiver to connect to the nearest vehicle *on the same road* as itself when there is at least one such vehicle within a distance of d_{th} from the receiver and on this road; otherwise it connects to the nearest MBS. As a result, safety messages are never propagated from one road to another. This forms the third and last scheme considered in this thesis.

2.6 Performance Metrics

In order to gauge the performance of cellular-assisted VANETs, the following metrics are used in this thesis:

1) Probability of Coverage:

The primary motivation behind taking cellular assistance is to improve the coverage at the vehicular nodes in the network. In this thesis, we ignore the effect of noise, so the Signal-to-Interference Ratio (SIR) is the deciding factor for coverage, i.e. a signal is successfully received when the SIR at the receiver crosses some predefined threshold T. Thus, the coverage probability is given by $\mathbb{P}_{cov} = \mathbb{P}[SIR > T]$. In this thesis, the expressions for coverage under different cellular-assisted VANET schemes are derived using tools from stochastic geometry, and then compared with results obtained using simulation. Note that coverage is expected to improve by using cellular assistance, especially under the maximum power-based scheme.

2) Association Probability:

Although connecting to the cellular network is expected to provide an improvement in coverage (especially under the maximum power-based scheme), it also increases the required throughput of the cellular network. This additional load obviously increases when the VANET connects to the cellular network more frequently; so, the VANET should aim to have as low a probability of connecting to the cellular network as possible. Thus, the probability of association with the nearest vehicle and with the nearest MBS, are both very important parameters that affect the network performance. Note that the sum of these two probabilities

is always 1. In this thesis, we analyze these association probabilities, especially the cellular association probability. Notably, one of the key design goals in this thesis is to increase the coverage probability in the vehicular network while also limiting the probability of connecting to the cellular network.

2.7 Key Assumptions

The next two chapters mathematically analyze the vehicular network and derive expressions for the tier association and coverage probabilities. The assumptions are summarized next for the ease of reference.

1. All the nodes in the same tier transmit at the same power: every vehicle transmits at $\frac{1}{\epsilon_v}$, while every cellular MBS has a transmit power of $\frac{1}{\epsilon_M}$. Power control is therefore not considered.

2. Rayleigh fading is assumed for all the wireless channels, i.e., fading coefficient $h \sim \exp(1)$.

3. The vehicles are all assumed to be located along certain *linear* roads in the network (modeled by a Poisson Line Process). Also, vehicles are located on each road with the same intensity μ. Extension to different vehicular intensities on different roads is straightforward.

4. We assume that the thermal noise at the receiver is negligible compared to the self interference. As a result, the signal to interference ratio (SIR) closely approximates signal to interference plus noise ratio (SINR). In this case, the coverage probability can be accurately defined in terms of the SIR.

Chapter 3

Distributions of Distances and

Interference

An intermediate step in evaluating the coverage probability at a typical vehicular node in the network is to

derive the distributions of the distances to the candidate serving nodes, which are the nearest cellular MBS

and the nearest vehicle to the typical node. These distributions are derived next.

3.1 Distances to Nearest VANET and Cellular Nodes (d_v, d_M)

The PDF of distance to the nearest vehicle (d_v) can be derived by obtaining an expression for its CDF, and

then differentiating it. The simplest method for finding the CDF $F_{d_v}(\rho)$ is to obtain the probability of there

being at least one vehicle inside a distance of ρ from the receiver. A similar approach can also be used to

find the PDF of distance to the nearest MBS. The results follow from basic properties of a PPP.

Lemma 2. *The distance d_v from the typical node to its nearest vehicle has the CDF*

$$F_{d_v}(\rho) = 1 - \exp\left[-2\pi\lambda \int\limits_{r=0}^{\rho} 1 - e^{-2\mu\sqrt{\rho^2-r^2}}\,\mathrm{d}r\right] e^{-2\mu\rho}, \tag{3.1}$$

and the PDF:

$$f_{d_v}(\rho) = -2\mu\left[\exp\left(-2\pi\lambda\rho\int\limits_0^{\rho} e^{-2\mu\sqrt{\rho^2-r^2}}\,\mathrm{d}r\right) e^{-2\mu\rho}\right]$$
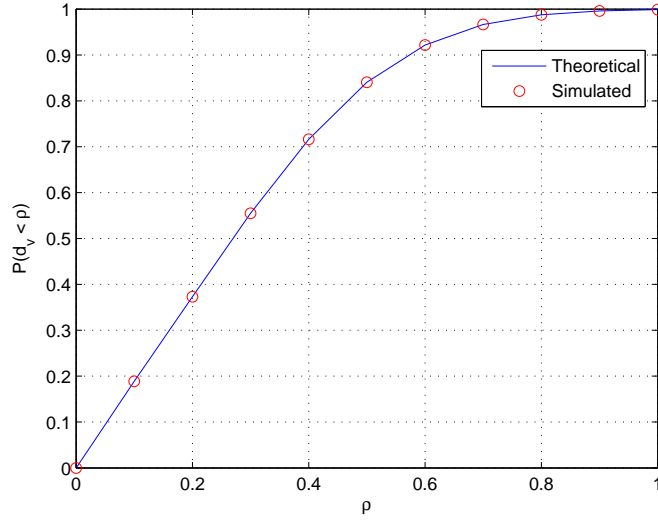
Figure 3.1: CDF of distance to nearest vehicle (for $\mu = 1, \lambda = 1$).

$$+ e^{-2\mu\rho} \int_0^\rho e^{-2\mu(\rho^2 - r^2)} \mathrm{d}r + e^{-2\mu\rho}(-2\pi\lambda\rho)\left[1 + \mu(1 - e^{-2\mu\rho})\right]. \tag{3.2}$$

Proof. In order to calculate the PDF of the distance d_v to the nearest vehicular node, let us calculate its CDF $F_{d_v}(\rho)$ first. The CDF can be calculated by conditioning over the number of roads n in the disk $b(o, \rho)$, and calculating the probability that at least one node exists on one of these road segments inside the disk.

$$F_{d_v}(\rho) = \mathbb{P}[d_v \leq \rho] = 1 - \mathbb{P}[d_v > \rho]$$

$$\overset{(a)}{=} 1 - \mathbb{P}[N_v(o, \rho) = 0]\mathbb{P}[N_{v0}(-\rho, \rho) = 0]$$

$$\overset{(b)}{=} 1 - \exp\left[-2\pi\lambda \int_{r=0}^\rho 1 - e^{-2\mu\sqrt{\rho^2 - r^2}} \mathrm{d}r\right] e^{-2\mu\rho}$$

where (a) follows from the fact that the event $d_v > \rho$ occurs when both of the following independent events occur: (i) there is no vehicle on $\Phi \setminus \{D_0\}$ in the ball $b(o, \rho)$, and (ii) there are no vehicles in D_0 in $[-\rho, +\rho]$. The probability of the first event has already been derived in Lemma 1, while that of the second part is $e^{-2\mu\rho}$; these are directly applied to obtain step (b). The PDF can now be calculated as follows:

$$f_{d_v}(\rho) = \frac{\mathrm{d}}{\mathrm{d}\rho}\left(1 - \exp\left[-2\pi\lambda\rho \int_{r=0}^\rho 1 - e^{-2\mu\sqrt{\rho^2 - r^2}} \mathrm{d}r\right] e^{-2\mu\rho}\right)$$

$$= -\frac{\mathrm{d}}{\mathrm{d}\rho}\exp\left[-2\pi\lambda\rho \int_{r=0}^\rho (1 - e^{-2\mu\sqrt{\rho^2 - r^2}} \mathrm{d}r)\right] e^{-2\mu\rho}$$

19

$$\overset{(a)}{=} -2\mu \left[\exp \left(-2\pi\lambda\rho \int_0^\rho e^{-2\mu\sqrt{\rho^2 - r^2}} \mathrm{dr} \right) e^{-2\mu\rho} \right]$$

$$+ e^{-2\mu\rho} \int_0^\rho e^{-2\mu(\rho^2 - r^2)} \mathrm{dr} + e^{-2\mu\rho}(-2\pi\lambda\rho) \left[1 + \mu(1 - e^{-2\mu\rho}) \right], \tag{3.3}$$

where step (a) is obtained using the Leibniz rule for differentiating over an integral. □

Now, for completeness, we state the distribution of the distance from a typical point to the closest MBS, which simply follows from the null probability of a PPP [6].

Lemma 3. *The distance d_M to the nearest MBS from a typical vehicle has the CDF ad PDF:*

$$\text{CDF:} \ \ F_{d_M}(\rho) = 1 - e^{-\pi\lambda_a\rho^2} \tag{3.4}$$

$$\text{PDF:} \ \ f_{d_M}(\rho) = 2\pi\lambda_a\rho e^{-\pi\lambda_a\rho^2}. \tag{3.5}$$

Proof. The CDF of the distance d_M to the nearest MBS is denoted by $F_{d_M}(\rho) = \mathbb{P}(d_M \leq \rho)$; this is equivalent to the probability that at least one MBS exists in the disk $b(o, \rho)$.

$$F_{d_M}(\rho) = 1 - \mathbb{P}[N_M(o, \rho) = 0]1 - e^{-\pi\lambda_a\rho^2}.$$

The PDF can now be derived by differentiating the CDF, which completes the proof. □

3.2 Laplace Transform of Interference

As will be evident in the next chapter, the next intermediate step in calculating the coverage probability is to analyze the interference originating from all the nodes in the network (except the serving node). In this section, we first introduce the general expression for Laplace transform of interference in the presence of Rayleigh fading, and then proceed to apply it and derive the expression for cellular-assisted VANETs.

3.2.1 Laplace Transform of Interference Under Rayleigh Fading

As shown in the next chapter, the coverage probability in the presence of Rayleigh fading simply reduces to the Laplace transform of interference I. The Laplace transform $\mathcal{L}_I(s)$ is defined as

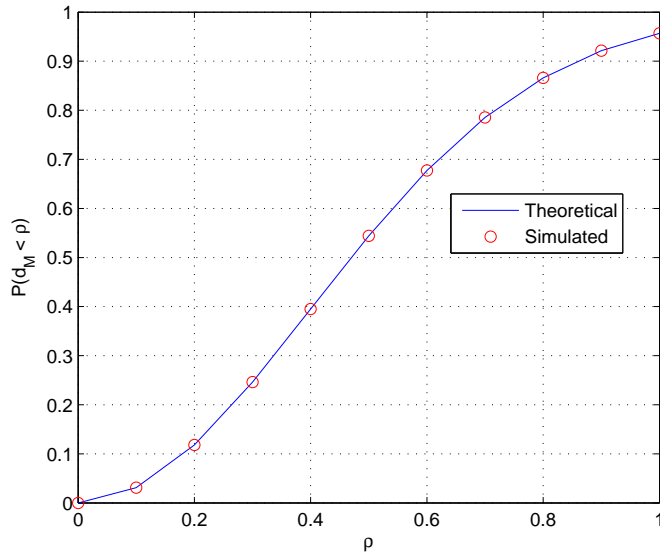$$\mathcal{L}_I(s) \triangleq \mathbb{E}\left[e^{-sI}\right] \tag{3.6}$$

Figure 3.2: CDF of distance to nearest MBS (for $\mu = 1, \lambda = 1$).

For a wireless network with interference field modeled as a PPP Φ, where each node transmits at the same power $1/\epsilon$ and all wireless channels suffer from independent Rayleigh fading (i.e., $h_x \sim \exp(1)$), the *conditional* Laplace transform (conditioned on the locations of the interferers) can be evaluated easily as [6]

$$\mathcal{L}_I(s) = \mathbb{E}\left[\exp\left(-\sum_{x \in \Phi} \frac{s}{\epsilon} h_x \|x\|^{-\alpha}\right)\right] = \mathbb{E}\left[\prod_{x \in \Phi} \mathbb{E}_{h_x} \exp\left(-\frac{s}{\epsilon} h_x \|x\|^{-\alpha}\right)\right] = \mathbb{E}\left[\prod_{x \in \Phi} \frac{1}{1 + \frac{s}{\epsilon}\|x\|^{-\alpha}}\right], \quad (3.7)$$

where the last step now simply follows by taking expectation over $h_x \sim \exp(1)$. Note that the above expression is a *conditional* Laplace transform because we haven't yet averaged over the locations of the interferers. Now using this basic result, we characterize the interference in a cellular-assisted VANET next.

3.2.2 Interference in Cellular-Assisted VANETs

Note that in the Cellular-Assisted Vehicular Network, the interference at a typical node originates from the following three *independent* sources:

i) Vehicular nodes on all other roads in $\mathbb{R}^2$. Let this network be denoted by Φ_v.

ii) Vehicular nodes on the same road (denoted by Φ_r).

iii) The cellular MBSs (Φ_M).

Thus, the Laplace interference of the total interference in the network can be obtained by characterizing

21

the interference from each independent source. The expression for the interference from all other roads in the network (point (i) above) can be derived directly from Equation 3.7. However, it is to be noted that the interfering nodes in Φ_v are not located through the entirety of $\mathbb{R}^2$. Their locations are, in fact, constrained based on the cellular-assisted VANET scheme being used, as well as on the type of transmitter being connected to. So, the final expression for the Laplace transform of interference will depend on these constraints on the interfering node locations. This also holds true for the other two sources of interference; the equations for their Laplace transform need to reflect the constraints of node locations as well. For instance, when we know that the typical node is being served by the closest point of a PPP, this implies that there can be no interfering nodes closer to the typical point than the serving node [16]. This introduces *exclusion zones* in the interference field, which are studied next.

Spatial Distribution of Interferers: Exclusion Zones

Note that since the receiver always connects to the nearest vehicle or MBS, interfering nodes are not present everywhere in $\mathbb{R}^2$; for example, as illustrated in Figure 3.3, if the receiver connects to the nearest MBS at a distance of d_M from itself, all interfering MBSs must be located at distances greater than d_M from it. As a result, there exist *exclusion zones* for each type of transmitter (vehicle and MBS) in which no interferer of that type is present. Since the size and location of these exclusion zones affect the distribution of interfering nodes, and hence the interference itself, we need to formally define these zones in order to chatacterize the total interference and the coverage probability at a receiving node in the network.

So, we define some distances r_v, r_r and r_M, which are the minimum possible distances from the receiver to the closest possible interfering vehicle on other roads, closest possible interfering vehicle on the same road, and closest possible interfering MBS, respectively. As will be evident in the sequel, these distances depend not only on the distance to the nearest transmitter, but also on the cellular-assisted VANET scheme being used and on the type of transmitter being connected to.

The regions $b(o, r_v)$, $[-r_r, +r_r]$ and $b(o, r_M)$ are thus the exclusion zones for Φ_v, Φ_r and Φ_M respectively. Since no interference originates from these exclusion zones, the interference from the three independent sources can be compactly represented by the following notation:
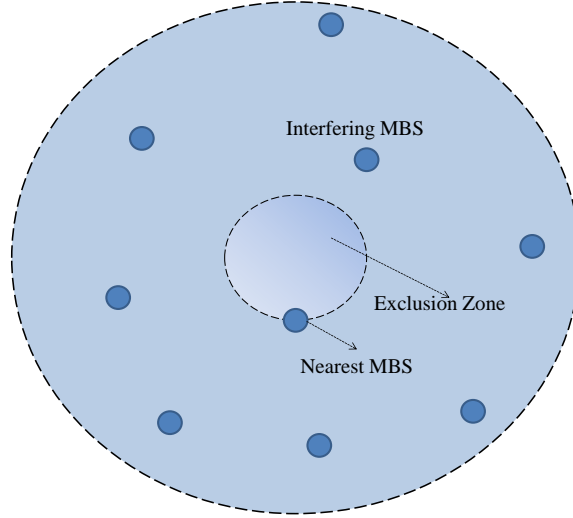
Figure 3.3: Exclusion Zones for Interfering MBSs.

$$I_v = I[\Phi_v \cap b(o, r_v)^C] \tag{3.8}$$

$$I_r = I[\Phi_r \cap [-r, +r]^C] \tag{3.9}$$

$$I_M = I[\Phi_M \cap b(o, r_M)^C] \tag{3.10}$$

where $I[\Phi]$ denotes the interference originating from a PPP Φ, and B^C is the complement of region B.

We shall now calculate the Laplace transform of these individual interference terms, which will completely characterize the interference originating from all three sources discussed above.

3.2.3 Interference from vehicles on other roads $(\mathcal{L}_{I_v}(s))$

In order to calculate $\mathcal{L}_{I_v}(s)$, we first find the Laplace transform of interference from a single road, at a *perpendicular* distance r from o. The distance of a point x from the mid-point of its line segment is denoted by t, thus its distance from o is given by $||x|| = \sqrt{r^2 + t^2}$ (See Figure 3.4 for details).

Lemma 4. *The Laplace transform of interference at a typical node, originating from a single road at a*

Figure 3.4: Distribution of interferers on lines falling inside and outside the exclusion zones.

distance r, is:
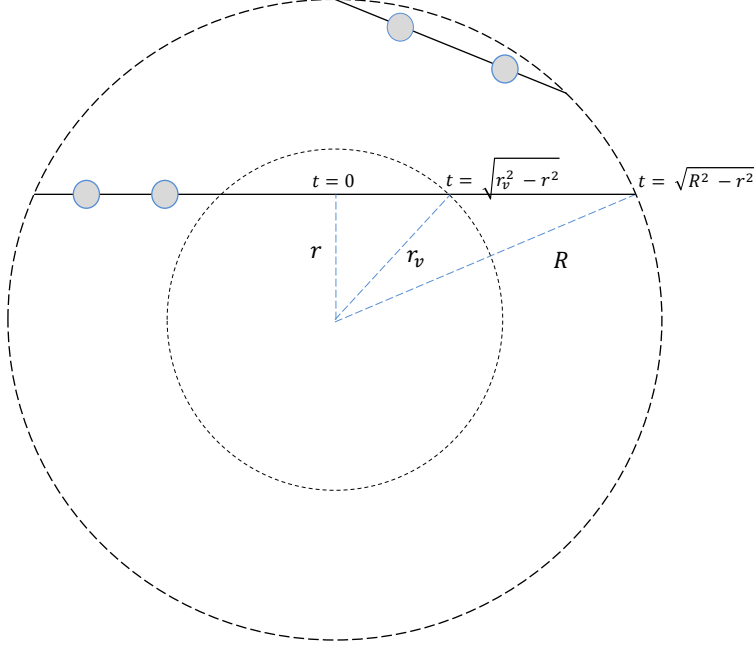
$$\mathcal{L}_I(s) = \begin{cases} g_1(r) = \exp\left[-2\mu \int\limits_{t=0}^{\sqrt{R^2-r^2}} 1 - \frac{1}{1+\frac{s}{\epsilon}(r^2+t^2)^{-\alpha/2}}\mathrm{dt}\right], r \geq r_v \\ g_2(r) = \exp\left[-2\mu \int\limits_{t=\sqrt{r_v^2-r^2}}^{\sqrt{R^2-r^2}} 1 - \frac{1}{1+\frac{s}{\epsilon}(r^2+t^2)^{-\alpha/2}}\mathrm{dt}\right], r < r_v. \end{cases} \tag{3.11}$$

Proof. Figure 3.4 shows a disk containing two roads: one at a distance $r \geq r_v$, which entirely lies outside the exclusion zone (let us denote this road by D_1), and one at $r < r_v$ (denoted by D_2). While interferers could be located anywhere on D_1, the road D_2 can have interferers lying only in the regions $t = \left(-\sqrt{R^2-r^2}, -\sqrt{R^2-r_v^2}\right)$ and $t = \left(\sqrt{R^2-r_v^2}, \sqrt{R^2-r^2}\right)$. We treat these two roads separately.

The Laplace transform of interference from D_2 can be calculated by conditioning over the number of points on that line which lie inside a disk of radius R. Note that for a line at a distance r from the center, the length of its segment lying inside this disk is given by $2\sqrt{R^2-r^2}$. So, by using the properties of a PPP, the probability of there being m points in this segment is given by $e^{-2\mu\sqrt{R^2-r^2}}\frac{\left(2\mu\sqrt{R^2-r^2}\right)^m}{m!}$. Now, we can proceed to find the Laplace transform of total interference by finding that of the interference originating

from each individual point in the segment. So, $\forall r \geq r_v$,

$$g_1(r) \stackrel{(a)}{=} E\left[\prod_{x \in D_r} \frac{1}{1 + \frac{s}{\epsilon}||x||^{-\alpha}}\right]$$

$$\stackrel{(b)}{=} \sum_{m \geq 0} P[N = m]\left(\int_{t=-\sqrt{R^2-r^2}}^{+\sqrt{R^2-r^2}} \frac{1}{1 + \frac{s}{\epsilon}(r^2 + t_1^2)^{-\alpha/2}} f(t)\mathrm{dt}\right)^m$$

$$\stackrel{(c)}{=} \sum_{m \geq 0} e^{-2\mu\sqrt{R^2-r^2}} \frac{(2\mu\sqrt{R^2 - r^2})^m}{m!(2\sqrt{R^2 - r^2})^m}\left(\int_{-\sqrt{R^2-r^2}}^{+\sqrt{R^2-r^2}} \frac{\mathrm{dt}}{1 + \frac{s}{\epsilon}(r^2 + t^2)^{-\alpha/2}}\right)^m$$

$$\stackrel{(d)}{=} e^{-2\mu\sqrt{R^2-r^2}} \sum_{m \geq 0} \frac{\mu^m\left[2\int_{t=0}^{+\sqrt{R^2-r^2}}\left(\frac{1}{1+\frac{s}{\epsilon}(r^2+t^2)^{-\alpha/2}}\right)\right]^m \mathrm{dt}}{m!}$$

$$\stackrel{(e)}{=} e^{-2\mu\sqrt{R^2-r^2}} \exp\left[2\mu\int_{t=0}^{+\sqrt{R^2-r^2}}\left(\frac{1}{1+\frac{s}{\epsilon}(r^2+t^2)^{-\alpha/2}}\right)\mathrm{dt}\right]$$

$$\stackrel{(f)}{=} \exp\left[-2\mu\int_{t=0}^{\sqrt{R^2-r^2}} 1 - \frac{1}{1 + \frac{s}{\epsilon}(r^2 + t^2)^{-\alpha/2}}\mathrm{dt}\right],$$

where (a) has already been defined in Equation 3.6 as the expression for the Laplace transform of interference in any network with Rayleigh fading: in this case, a road D_r at a distance r from o (its intersection with a disk of radius R thus has a length of $2\sqrt{R^2 - r^2}$). In the next step (b), we condition over the number of points N and decondition over its all possible values from $[0, \infty]$. Note that we make use of the fact that the value of t for the different points are iid random variables. Step (c) is derived from the fact that the number of points on the line segment of length $2\sqrt{R^2 - r^2}$ is a Poisson random variable with mean $2\mu\sqrt{R^2 - r^2}$, while t for each point is uniformly distributed between $[-\sqrt{R^2 - r^2}, +\sqrt{R^2 - r^2}]$ and has a pdf $f(t) = \frac{1}{2\sqrt{R^2-r^2}}$. We get (d) from the property of integral of even functions, while (e) is derived from the Taylor Series expression for e^x. Finally, expression (f) is obtained by the property $\int_{t=0}^{x} \mathrm{dt} = \mathrm{x}$. This completes the proof for $r \geq r_v$.

As has already been noted, for any line at a distance $r < r_v$ from o (for example D_1), there are no interfering nodes in the region $t = [-\sqrt{r_v^2 - r^2}, +\sqrt{r_v^2 - r^2}]$, so the values for t can now vary only from $[-\sqrt{R^2 - r^2}, -\sqrt{r_v^2 - r^2}]$ and $[\sqrt{r_v^2 - r^2}, \sqrt{R^2 - r^2}]$. Thus, the limits of integration will change from $[0, \sqrt{R^2 - r^2}]$ to $[\sqrt{r_v^2 - r^2}, \sqrt{R^2 - r^2}]$, as follows:

$$g_2(s, r, r_v) = \exp\left[-2\mu\int_{t=\sqrt{r_v^2-r^2}}^{\sqrt{R^2-r^2}} 1 - \frac{1}{1 + \frac{s}{\epsilon}(r^2 + t^2)^{-\alpha/2}}\mathrm{dr}\right], \forall r < r_v. \tag{3.12}$$

This completes the proof for the other part $(r < r_v)$ as well. □

Thus, we have derived the Laplace transform of interference originating from the nodes on any single road in the network. This result will now be used to characterize the interference originating from the entire vehicular network, by conditioning over the number of roads N_{roads}, and obtaining the Laplace transform of total interference as a product of the Laplace transforms of interference from these individual roads.

Lemma 5. *At a typical vehicular node, the Laplace transform of total interference originating from all other roads in the network is given by:*

$$\mathcal{L}_{I_v}(s, r_v) = \exp\left[-2\pi\lambda\left(\int_{r=0}^{r_v}(1 - g_1(r))dr + \int_{r=r_v}^{R}(1 - g_2(r))\right)dr\right]. \tag{3.13}$$

Proof. In order to calculate the Laplace transform of the total interference originating from a Poisson line process, we condition on the number of lines n that intersect a disk of radius R. Then we use this to find the Laplace transform of interference originating from all these roads, by using the expression for $\mathcal{L}_I(s)$ for one road (derived in Lemma 4). Recall from Lemma 4 that the expression for $\mathcal{L}_I(s)$ is different for $r < r_v$ and $r > r_v$. The Laplace transform can be found as

$$\mathcal{L}_I(s) = E\left[e^{-sI}\right] = E\left[e^{-sE\left[\sum_{x\in\Phi_v} I_r(x)\right]}\right] = E\left[\prod_{x\in\Phi_v} e^{-sE[I_r(x)]}\right]$$

$$\stackrel{(a)}{=} \left[\sum_{j\geq 0}\frac{e^{-2\pi r_v\lambda}(2\pi r_v\lambda)^j}{j!(2R)^j}\int_{r=-r_v}^{+r_v}[g_1(r)]^j dr\right]\left[\sum_{k\geq 0}\frac{e^{-2\pi\rho\lambda}(2\pi(R-r_v)\lambda)^k}{k!(2(R-r_v))^k}2\int_{r=r_v}^{R}[g_2(r)]^k dr\right]$$

$$\stackrel{(b)}{=} \exp\left[-2\pi\lambda\left(\int_{r=0}^{r_v}(1 - g_1(r))dr + \int_{r=0}^{r_v}(1 - g_2(r))dr\right)\right]. \tag{3.14}$$

In step (a), we condition over the number of lines j crossing the region $b(o, r_v)$ (this is a Poisson random variable with mean $2\pi\lambda r_v$) and on k, the number of lines lying between the disks $b(o, R)$ and $b(o, r_v)$, which is another Poisson random variable with mean $2\pi(R - r_v)$. Note that the corresponding PPPs for these two regions are independent of each other, and hence we can analyze these two separately. The value of r (distance to the receiver) for the lines in either region is i.i.d and uniformly distributed. (b) is simply derived by using the Taylor series expression for e^x, and by the property of $\int_0^R dr = R$. Note that the expression for $\mathcal{L}_{I_v}(s, r_v)$ can be calculated by subsituting the values of $g_1(r)$ and $g_2(r)$ derived in Lemma 4, into Equation 3.13. This completes the proof. □

3.2.4 Interference from vehicles on the same road $(\mathcal{L}_{I_r}(s))$

Now, we proceed to Φ_r, the second source of interference, which consists of the vehicles on the same road as the one in which the receiver is located. We shall now calculate the Laplace transform of interference originating from this road.

Lemma 6. *The total interference originating from all nodes on the same road as the receiver has the following Laplace transform:*

$$L_{I_r}(s, a_r) = \exp\left[-2\mu \int_{t=r_r}^{R} 1 - \frac{1}{1 + \frac{s}{\epsilon_v} t^{-\alpha}} \mathrm{dt}\right]. \tag{3.15}$$

Proof. The Laplace transform of interference originating from nodes on a single road have already been derived in Lemma 4. Also, $r = 0$ for the road passing through o. Thus, the Laplace transform of interference from all the nodes on this road can be calculated simply by substituting $r = 0$ and $r_v = r_r$ in Lemma 4. $\quad\square$

3.2.5 Interference originating from MBSs $(\mathcal{L}_{I_M}(s))$

The expression for $\mathcal{L}_{I_M}$ for the interference originating from a 2D PPP of cellular MBSs is well known, e.g. see [6], and is given by:

$$\mathcal{L}_{I_M}(s, r_M) = \exp\left[-\lambda(\pi s^\delta \Gamma(1 + \delta)(1 - \delta) - \pi r_M^2 H_\delta(r_M^\alpha/s))\right] \tag{3.16}$$

where H is the Gauss hypergeometric function and $\delta = 2/\alpha$. Note that for $\alpha = 4$, $H_{1/2}(x) = \sqrt{x}\arctan(1/\sqrt{x})$.

Now, we have the expressions for Laplace transform of each individual type of interference. The total interference at o is given by the sum of these three sources, i.e.

$$I = I_v + I_r + I_M \tag{3.17}$$

Since these three interference sources are independent of each other, the Laplace transform of the total interference is simply the product of their individual Laplace transforms, i.e.:

$$\mathcal{L}_I(s, r_v, r_r, r_M) = \mathcal{L}_{I_v}(s, r_v)\mathcal{L}_{I_r}(s, r_r)\mathcal{L}_{I_M}(s, r_M) \tag{3.18}$$

The expressions for the individual terms in the RHS of Equation 3.18 have been mentioned in Equations 3.13, 3.15 and 3.16 respectively. Their product gives the expression for Laplace transform of total interference at a typical node, which will now be used to calculate coverage probability in the next chapter.

Chapter 4

Coverage Probability

In this chapter, we shall use the expressions for interference and inter-node distances, obtained in Chapter 3, to derive expressions for coverage probability at a typical node in a cellular-assisted VANET. While the aforementioned expressions generally hold true for any PLP in $\mathbb{R}^2$ overlapped with a 2D PPP, the expressions derived in this chapter depend on the network scenario, i.e. on the specific cellular-assisted VANET scheme being used by the network. We shall first derive a general expression for the coverage probability, and then proceed to apply it to networks using each of these different schemes.

In this thesis, we are using an SIR (Signal-to-Interference Ratio)-based coverage probability as the metric of interest, where a message is successfully detected by a receiver when the SIR crosses a predefined threshold T. Thus, for a network of interferers with power $\frac{1}{\epsilon}$, in which the nearest transmitter is at a distance of ρ from the receiver, the probability of coverage is given by:

$$\mathbb{P}_{cov} = \mathbb{P}[SIR > T] = \mathbb{P}\left[\frac{\frac{1}{\epsilon}h\rho^{-\alpha}}{I} > T\right] = \mathbb{P}\left[h > \epsilon T\rho^{\alpha}I\right] = \mathbb{E}\left[e^{-\epsilon T\rho^{\alpha}I}\right] = \mathcal{L}_I(\epsilon T\rho^{\alpha}).$$

Thus, the coverage probability in a Rayleigh fading network is given by the Laplace transform of interference ($\mathcal{L}_I(s)$, where $s = \epsilon T\rho^{\alpha}$). So, we can say that in the two-tier cellular-VANET, the coverage probability (conditioned for ρ and the type of transmitter Tx being connected to) is given by:

$$\mathbb{P}_{cov}|(Tx, \rho) = \mathcal{L}_{I_v}(\epsilon T\rho^{\alpha}, r_v)\mathcal{L}_{I_r}(\epsilon T\rho^{\alpha}, r_r)\mathcal{L}_{I_M}(\epsilon T\rho^{\alpha}, r_M) \tag{4.1}$$

Thus, the coverage probability for a particular type of transmitter (vehicle or MBS) can be obtained by

28

taking an expectation over ρ. Also, the exclusion zone boundaries r_v and r_M directly depend on the value of

ρ, so they can be expressed as $r_v(\rho)$ and $r_M(\rho)$. Thus, taking these two facts in consideration, the expression

for coverage probability for a particular type of transmitter (Tx) can be rewritten as:

$$\mathbb{P}_{cov}|Tx = \mathbb{E}_\rho[\mathcal{L}_{I_v}(\epsilon T\rho^\alpha, r_v(\rho))\mathcal{L}_{I_r}(\epsilon T\rho^\alpha, r_r(\rho))\mathcal{L}_{I_M}(\epsilon T\rho^\alpha, r_M(\rho))] \tag{4.2}$$

Note that using Equation 4.2, the coverage probability can now be directly calculated from the expressions

for: (i) the Laplace transform of each type of interference $(\mathcal{L}_{I_v}(s), \mathcal{L}_{I_r}(s) \text{and} \mathcal{L}_{I_M}(s))$, (ii) the PDF of the

distance ρ to the transmitter $(f_{d_v}(\rho), f_{d_r}(\rho), f_{d_M}(\rho))$, and (iii) the exclusion zone boundaries (r_v, r_r, r_M).

So, in order to compute the coverage probability for each cellular-Assisted VANET scheme, we shall

follow the following steps:

1) Calculate the Laplace transform of interference $\mathcal{L}_I(s)$. Replace s with $\epsilon T\rho^\alpha$ to find $\mathcal{L}_I(\epsilon T\rho^\alpha)$.

2) Find the pdf $f(\rho)$ of distance ρ of the typical node from the transmitter.

3) Find the coverage probability for each type of transmitter, using the formula

$\mathbb{P}_{cov}(\rho)|Tx = \mathbb{E}_\rho[\mathcal{L}_{I_v}(\epsilon T\rho^\alpha, r_v(\rho))\mathcal{L}_{I_r}(\epsilon T\rho^\alpha, r_r(\rho))\mathcal{L}_{I_M}(\epsilon T\rho^\alpha, r_M(\rho))]$.

4) Find the probabilities $\mathbb{P}_v(\rho)$ and $\mathbb{P}_{MBS}(\rho)$ of connecting to the nearest vehicle and MBS respectively.

5) Find the overall probability of coverage using the formula

$\mathbb{P}_{cov} = \int\limits_{\rho=0}^{\infty} \mathbb{P}_v(\rho)\mathbb{P}_{cov|v}(\rho) + \mathbb{P}_{MBS}(\rho)\mathbb{P}_{cov|MBS}(\rho)f(\rho)d\rho$.

As already mentioned, Steps 1 and 2 are agnostic of the type of celular-assisted VANET scheme being

used; also, both these steps have been completed in the last chapter. In this chapter, we focus on steps

3, 4 and 5, and derive an expression for coverage probability in the maximum power-based and threshold

distance-based cellular-assisted VANET schemes.

To compute the coverage probability for each scheme, we first find the expressions for coverage probability

for each type of transmitter ($\mathbb{P}_{cov|v}$ and $\mathbb{P}_{cov|MBS}$), and the probabilities $\mathbb{P}_v$ and $\mathbb{P}_{MBS}$ of connecting to these

types, and use it to find the overall coverage probability as follows:

$$\mathbb{P}_{cov} = \mathbb{E}_\rho[\mathbb{P}_v(\rho)\mathbb{P}_{cov|v}(\rho) + \mathbb{P}_{MBS}(\rho)\mathbb{P}_{cov|MBS}(\rho)] \tag{4.3}$$
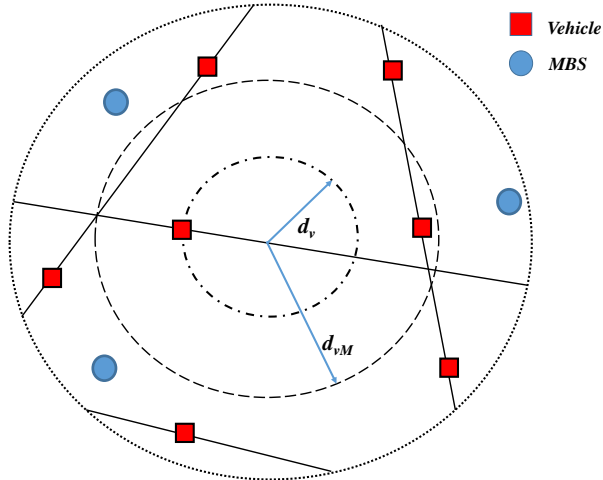
Figure 4.1: Scenario of connecting to a Vehicle in Maximum Average Power Based Scheme.

4.1 Maximum Average Power Based Scheme

In this scheme, the receiver aims to connect to the node from which it receives the strongest signal in terms of the average received power. The receiver selects the nearest vehicle and the nearest MBS, and chooses to receive data from the node which supplies a higher time-averaged power. If the averaging period is significantly large compared to the channel coherence time, the average power will be independent of fading (and given by $\frac{1}{\epsilon}||x||^{-\alpha}$). The association probabilities for this scheme are computed next.

4.1.1 Association Probabilities ($\mathbb{P}_v$, $\mathbb{P}_{MBS}$)

As has already been mentioned, the coverage probability for the typical node changes based on which type of transmitter it connects to. So, in order to calculate the overall coverage probability, it is necessary to first find the probability of connecting to each individual type of transmitter. In this section, we shall calculate these probabilities conditioned on the value of ρ, i.e., the probabilities of the transmitting node being a vehicle or an MBS, given that it is at a distance of ρ from the receiver.

Lemma 7. *If the transmitter being connected to is at a distance of ρ, the probability of it being a vehicle is*

$$\mathbb{P}_v = \exp\left(-\lambda_a \pi \rho^2 \left(\frac{\epsilon_v}{\epsilon_M}\right)^{2/\alpha}\right). \tag{4.4}$$

Proof. A receiving vehicle connects to the nearest vehicle when the average received power from it is greater

than that from the nearest MBS. So, if the nearest vehicle and base stations are at a distance of d_v and d_M respectively, the probability of this event occuring is given by:

$$\mathbb{P}\left[(1/\epsilon_v)d_v^{-\alpha} > (1/\epsilon_M)d_M^{-\alpha}\right] = \mathbb{P}\left[d_M > d_v(\frac{\epsilon_v}{\epsilon_M})^{\frac{1}{\alpha}}\right] \tag{4.5}$$

For notational simplicity, let $d_{vM} = d_v(\frac{\epsilon_v}{\epsilon_M})^{\frac{1}{\alpha}}$. So, a receiving vehicle at o connects to the closest transmitting vehicle when no MBSs exist in the ball $b(o, d_{vM})$. The probability of this happening is:

$$\mathbb{P}_v(d_v) = \exp(-\lambda_a \pi d_{vM}^2) \tag{4.6}$$

Since the receiver connects to the nearest vehicle, so $d_v = \rho$ above, which completes the proof. $\square$

$\mathbb{P}_v(\rho)$ is the probability that the nearest transmitter is a vehicle, given that this transmitter is located at a distance of ρ from the receiver. Now we compute the association probability for MBSs.

Lemma 8. *The probability of a node connecting to a cellular MBS is:*

$$P_{MBS}(d_M) = \exp\left[-2\pi\lambda \int_{r=0}^{d_{vM}} e^{-\mu\sqrt{\rho^2((\frac{\epsilon_M}{\epsilon_v})^{\frac{2}{\alpha}} - r^2)}} dr\right] e^{-2\mu\rho(\frac{\epsilon_M}{\epsilon_v})^{\frac{1}{\alpha}}}$$

Proof. If the nearest MBS is at a distance d_M away, the receiver connects to it only when there are no vehicles in the region $b(0, d_{Mv})$, where $d_{Mv} = d_M(\frac{\epsilon_M}{\epsilon_v})^{\frac{1}{\alpha}}$. Therefore,

$$\mathbb{P}_{MBS}(d_M) \overset{(a)}{=} \mathbb{P}\left[N_v(b(o, d_{Mv})) = 0\right] \overset{(b)}{=} \exp\left[-2\pi\lambda \int_{r=0}^{d_{vM}} e^{-\mu\sqrt{d_{Mv}^2 - r^2}} dr\right] e^{-2\mu d_{vM}}, \tag{4.7}$$

where $d_{Mv} = d_M(\frac{\epsilon_M}{\epsilon_v})^{\frac{1}{\alpha}} \overset{(c)}{=} \rho(\frac{\epsilon_M}{\epsilon_v})^{\frac{1}{\alpha}}$. Step (a) follows from the fact that the receiver connects to the nearest MBS when no vehicles exist in the ball $b(o, d_{vM})$. (b) is derived from Lemma 1. We can write step (c) because when the receiver connects to the nearest MBS, then the distance to the transmitter is given by $\rho = d_M$. Therefore, after making this substitution, we get

$$\mathbb{P}_{MBS}(\rho) = \exp\left[-2\pi\lambda \int_{r=0}^{d_{vM}} e^{-\mu\sqrt{(\rho\frac{\epsilon_v}{\epsilon_M})^{\frac{2}{\alpha}} - r^2}} dr\right] e^{-2\mu_v\rho(\frac{\epsilon_v}{\epsilon_M})^{\frac{1}{\alpha}}}, \tag{4.8}$$

which completes the proof. $\square$

When the nearest transmitter is at a distance of ρ from the receiver, $P_{MBS}(\rho)$ is the probability that this transmitter is a cellular MBS. We now study the exclusion zones for this case.

4.1.2 Exclusion Zones

When the receiver connects to the nearest vehicle (at a distance $\rho = d_v$), there are no interfering vehicles in the region $b(o, \rho)$ or on the same road in $[-\rho, +\rho]$. Also, the nearest MBS must be at a distance of at least $\rho(\frac{\epsilon_v}{\epsilon_M})^{\frac{1}{\alpha}}$, since the average power from it is less than that from the nearest vehicle.

Lemma 9. *In the maximum average power-based scheme, when the receiver connects to the nearest vehicle, there exist no interfering vehicles on other roads, vehicles on the same road, and cellular MBSs within a distance of r_v, r_r and r_M respectively, where:*

$$r_v = \rho, r_r = \rho, r_M = \rho \left(\frac{\epsilon_v}{\epsilon_M} \right)^{\frac{1}{\alpha}}. \tag{4.9}$$

When the receiver connects to the nearest MBS, the interfering vehicles are all at a distance of at least $\rho(\frac{\epsilon_M}{\epsilon_v})^{\frac{1}{\alpha}}$ from it. Also, all interfering MBSs lie outside the disk $b(o, \rho)$.

Lemma 10. *The exclusion zone boundaries in maximum average power-based scheme, when the receiver connects to nearest MBS, are given by:*

$$r_v = \rho \left(\frac{\epsilon_M}{\epsilon_v} \right)^{\frac{1}{\alpha}}, r_r = \rho \left(\frac{\epsilon_M}{\epsilon_v} \right)^{\frac{1}{\alpha}}, r_M = \rho \tag{4.10}$$

These expressions for the exclusion zone boundaries can now be applied to find the coverage probability.

4.1.3 Probability of Coverage for each type of Transmitter

The coverage probability when the receiver connects to each type of transmitter, has been derived in Equation 4.2. We shall use the values of the exclusion zone boundaries r_v, r_r and r_M to find the expression for coverage probability in the maximum average power-based scheme. The result is given next.

Lemma 11. *The probability of coverage when the receiver connects to the nearest **vehicle**, located at a distance of ρ, is:*

$$P_{cov|v}(\rho) = \mathcal{L}_{I_v} \left(\epsilon_v T \rho^\alpha, \rho \right) \mathcal{L}_{I_r} \left(\epsilon_v T \rho^\alpha, \rho \right) \mathcal{L}_{I_M} \left(\epsilon_v T \rho^\alpha, \rho (\frac{\epsilon_M}{\epsilon_v})^{\frac{1}{\alpha}} \right) \tag{4.11}$$

Lemma 12. *The probability of coverage at the receiver when it connects to the nearest **MBS**, at a distance of ρ, is:*

$$P_{cov|MBS}(\rho) = \mathcal{L}_{I_v} \left(\epsilon_M T \rho^\alpha, \rho (\frac{\epsilon_v}{\epsilon_M})^{\frac{1}{\alpha}} \right) \mathcal{L}_{I_r} \left(\epsilon_M T \rho^\alpha, \rho (\frac{\epsilon_v}{\epsilon_M})^{\frac{1}{\alpha}} \right) \mathcal{L}_{I_M} \left(\epsilon_M T \rho^\alpha, \rho \right) \tag{4.12}$$

Note that the expressions for $\mathcal{L}_{I_v}$, $\mathcal{L}_{I_r}$ and $\mathcal{L}_{I_M}$ have already been derived in Equations 3.13, 3.15 and 3.16, and can be directly applied to Lemmas 4.11 and 4.12 to obtain the coverage probabilities.

4.1.4 Probability of Coverage: Final Expression

The expression for probability of coverage can now be obtained directly from Equation 4.3, using the coverage probabilities for each individual type of transmitter (which were just derived in Lemmas 11 and 12), as follows.

Theorem 1. *The probability of coverage at a receiving node in an cellular-Assisted VANET, when it operates in the maximum average power-based mode, is given by:*

$$
\mathbb{P}_{cov} = \int_{\rho=0}^{\infty} \exp\left[-\lambda_a \pi \rho^2 \left(\frac{\epsilon_v}{\epsilon_M}\right)^{\frac{2}{\alpha}}\right] \mathcal{L}_{I_v}(\epsilon_v T \rho^\alpha, \rho) \mathcal{L}_{I_r}(\epsilon_v T \rho^\alpha, \rho) \mathcal{L}_{I_M}(\epsilon_v T \rho^\alpha, \rho(\frac{\epsilon_v}{\epsilon_M})^{\frac{1}{\alpha}}) f_{d_v}(\rho)\mathrm{d}\rho
$$

$$
+ \int_{\rho=0}^{\infty} \exp\left[-2\pi\lambda \int_{r=0}^{(\rho\frac{\epsilon_M}{\epsilon_v})^{1/\alpha}} e^{-\mu\sqrt{\rho^2(\frac{\epsilon_M}{\epsilon_v})^{2/\alpha}-r^2}}\mathrm{d}r\right] e^{-2\mu\rho(\frac{\epsilon_M}{\epsilon_v})^{1/\alpha}}
$$

$$
\mathcal{L}_{I_v}\left(\epsilon_v T \rho^\alpha, \rho\left(\frac{\epsilon_M}{\epsilon_v}\right)^{\frac{1}{\alpha}}\right) \mathcal{L}_{I_r}\left(\epsilon_v T \rho^\alpha, \rho\left(\frac{\epsilon_M}{\epsilon_v}\right)^{\frac{1}{\alpha}}\right) \mathcal{L}_{I_M}\left(\epsilon_v T \rho^\alpha, \rho\right) f_{d_M}(\rho)\mathrm{d}\rho \tag{4.13}
$$

As already noted, the expressions for the individual Laplace transforms, as well as the PDFs of the distance ρ to the nearest vehicle and MBS, have been derived in Chapter 3, and can be directly substituted in the above expression to obtain the final expression for coverage probability in the maximum average power-based scheme. We will revisit this result in the next Chapter.

4.2 Threshold Distance Based Scheme: Inter-Road

In this section, we analyze the coverage probability in the threshold distance scheme. As has been already noted, in this scheme the receiver chooses to connect to the nearest vehicle as long as there is at least one within a threshold distance away from the typical vehicle. Similar to the maximum average power based scheme, we shall find the expressions for association probabilities, interferer distributions and interference Laplace transforms, and use them to find the overall expression for coverage probability.

4.2.1 Association Probabilities

Lemma 13. *In the threshold distance-based scheme, the probability that a receiver connects to the nearest transmitting vehicle is given by:*

$$\mathbb{P}_v = 1 - \exp\left[-2\pi\lambda \int\limits_{r=0}^{d_{th}} e^{-\mu\sqrt{d_{th}^2-r^2}}\mathrm{d}r\right] e^{-2\mu d_{th}} \tag{4.14}$$

Proof. A receiver connects to the nearest vehicle whenever there is at least one vehicle inside a distance of d_{th} from itself. The probability of this occurring is:

$$\mathbb{P}_v = 1 - \mathbb{P}[N(b(o,d_{th})) = 0]\mathbb{P}[N(-d_{th}, +d_{th}) = 0] \overset{(a)}{=} 1 - \exp\left[-2\pi\lambda \int\limits_{r=0}^{d_{th}} e^{-\mu\sqrt{d_{th}^2-r^2}}\mathrm{d}r\right] e^{-2\mu d_{th}}, \tag{4.15}$$

where (a) is obtained from Lemma 1, by replacing R with d_{th} to find the null probability of there being no vehicles in the ball $b(0, d_{th})$. □

Lemma 14. *The probability of connecting to the nearest vehicle is:*

$$\mathbb{P}_{MBS} = \exp\left[-2\pi\lambda \int\limits_{r=0}^{d_{th}} e^{-\mu\sqrt{d_{th}^2-r^2}}\mathrm{d}r\right] e^{-2\mu d_{th}}. \tag{4.16}$$

Proof. When there are no vehicles inside the threshold distance, the receiver connects to the nearest MBS. The probability of this event can be obtained by using the null probability expression derived in Lemma 1:

$$\mathbb{P}_{MBS} = \mathbb{P}[N_v(b(o,d_{th})) = 0]\mathbb{P}[N_v(-d_{th}, +d_{th}) = 0] = \exp\left[-2\pi\lambda \int\limits_{r=0}^{d_{th}} e^{-\mu\sqrt{d_{th}^2-r^2}}\mathrm{d}r\right] e^{-2\mu d_{th}}. \tag{4.17}$$

In other words, $\mathbb{P}_{MBS}$ is simply $1 - \mathbb{P}_v$. This completes the proof. □

Thus, unlike the maximum power association policy discussed above, the probabilities of associating with the vehicles or the MBSs do not depend on the distance ρ to the transmitter in this case.

4.2.2 Exclusion Zones

Similar to the maximum power-based scheme, the exclusion zone boundaries for each type of transmitter vary based on whether the receiver connects to the nearest vehicle or to the nearest MBS.

Let us first look at the event in which the receiver connects to the nearest transmitting vehiecle. Naturally, if this vehicle is at a distance of ρ from the receiver, then all interfering vehicles must be at least at a distance

ρ from it. There is, however, no restriction on the location of interfering MBSs. The distance to them can vary anywhere in the range $[0, \infty)$. So, the exclusion zone boundaries are as follows:

$$r_v = r_r = \rho, r_M = 0. \tag{4.18}$$

When the receiver connects to the nearest MBS, it means that all vehicles (both on other roads and on the same road as the receiver) must be more than a distance d_{th} away. The distance to an interfering MBS is at least ρ, where ρ is the distance between the receiver and the transmitting MBS. In other words,

$$r_v = r_r = d_{th}, r_M = \rho. \tag{4.19}$$

4.2.3   Probability of Coverage for each type of Transmitter

As has been shown in Equation 4.2, the probability of coverage when the receiver connects to the two types of transmitters (vehicles and MBSs) are:

$$\mathbb{P}_{cov|v}(\rho) = \mathcal{L}_{I_v}(\epsilon_v T \rho^\alpha, \rho)\mathcal{L}_{I_r}(\epsilon_v T \rho^\alpha, \rho)\mathcal{L}_{I_M}(\epsilon_v T \rho^\alpha, 0), \tag{4.20}$$

$$\mathbb{P}_{cov|MBS}(\rho) = \mathcal{L}_{I_v}(\epsilon_v T \rho^\alpha, d_{th})\mathcal{L}_{I_r}(\epsilon_v T \rho^\alpha, d_{th})\mathcal{L}_{I_M}(\epsilon_v T \rho^\alpha, \rho). \tag{4.21}$$

Note that the expressions for $\mathcal{L}_{I_v}$, $\mathcal{L}_{I_r}$ and $\mathcal{L}_{I_M}$, have already been derived in Equations 3.13, 3.15 and 3.16.

4.2.4   Probability of Coverage: Final Expression

The expression for probability of coverage can now be derived directly by applying the expressions obtained in Equations 3.13, 3.15 and 3.16 to Equation 4.3, as follows:

Theorem 2. *The probability of coverage for a typical node in the cellular-assisted VANET, when it is operating in the threshold distance based mode is given by:*

$$\begin{aligned}
\mathbb{P}_{cov} &= \mathbb{E}_\rho[\mathbb{P}_v\mathbb{P}_{cov|v} + \mathbb{P}_{MBS}\mathbb{P}_{cov|MBS}] \\
&= \mathbb{P}_v \int_{\rho=0}^{\infty} \mathcal{L}_{I_v}(\epsilon_v T \rho^\alpha, \rho)\mathcal{L}_{I_r}(\epsilon_v T \rho^\alpha, \rho)\mathcal{L}_{I_M}(\epsilon_v T \rho^\alpha, 0)f_{d_v}(\rho)\mathrm{d}\rho \\
&\quad + \mathbb{P}_{MBS} \int_{\rho=0}^{\infty} \mathcal{L}_{I_v}(\epsilon_v T \rho^\alpha, d_{th})\mathcal{L}_{I_r}(\epsilon_v T \rho^\alpha, d_{th})\mathcal{L}_{I_M}(\epsilon_v T \rho^\alpha, \rho)f_{d_M}(\rho)\mathrm{d}\rho. \tag{4.22}
\end{aligned}$$

The expressions for $\mathbb{P}_v$, $\mathbb{P}_{MBS}$, $\mathcal{L}_{I_v}$ $\mathcal{L}_{I_M}$, $f_{d_v}(\rho)$ and $f_{d_M}(\rho)$ can be found in Equations 4.15, 4.17, 3.3 and 3.5 respectively, and can be directly applied to the above equation to obtain an expression for the overall coverage probability in the cellular-assisted VANET under the threshold distance-based scheme.

4.3 Intra-Road Communication

As we have already noted in this thesis, it may often be preferable to limit safety messaging to only between vehicles on the same road, so as to eliminate needless inter-road safety messages. In this section, we look at a scheme in which the receiver connects only to those transmitting vehicles which lie on D_0; if there are no vehicles within a threshold distance on this road, the receiver connects to the nearest cellular MBS, irrespective of the location of vehicles on the other roads.

4.3.1 Association Probabilities

The receiver connects to the nearest vehicle when there is at least one in the range $[-d_{th}, +d_{th}]$.

Lemma 15. *For the typical node, the probability of connecting to the nearest vehicle is:*

$$\mathbb{P}_v = 1 - e^{-2\mu d_{th}}. \tag{4.23}$$

Conversely, it connects to the nearest MBS when no vehicles lie in $[-d_{th}, +d_{th}]$.

Lemma 16. *For the typical node, the probability of connecting to the nearest MBS is:*

$$\mathbb{P}_{MBS} = e^{-2\mu d_{th}}. \tag{4.24}$$

4.3.2 Exclusion Zones

First, we look at the scenario in which the receiver connects to the nearest vehicle (at a distance ρ). In this case, there is no restriction on the possible locations of interfering vehicles on other roads, or on that of MBSs. However, interfering vehicles on D_0 must be further away than the serving node. Therefore

$$r_v = 0, r_r = \rho, r_M = 0. \tag{4.25}$$

When the transmitter being connected to is an MBS, it means that interfering vehicles on the same road are at least a threshold distance away, while those on other roads can be at any distance in the range $[0, R]$. Interfering MBSs must be at a minimum distance of ρ from the receiver.

$$r_v = 0, r_r = d_{th}, r_M = \rho \tag{4.26}$$

Note that r_v is always equal to zero in the intra-road communication scheme; since it operates completely independent of other roads in the network, there is no constraint on the location of vehicles on these roads.

4.3.3 Probability of Coverage for each type of Transmitter

Now, the expressions obtained for the interference Laplace transforms and exclusion zones can be used to obtain the expression for coverage probability for either type of transmitter, as follows:

$$\mathbb{P}_{cov|v} = \int_{\rho=0}^{d_{th}} \mathcal{L}_{I_v}(\epsilon_v T \rho^\alpha, 0) \mathcal{L}_{I_r}(\epsilon_v T \rho^\alpha, \rho) \mathcal{L}_{I_M}(\epsilon_v T \rho^\alpha, 0) 2\mu e^{-2\mu\rho} \mathrm{d}\rho, \tag{4.27}$$

$$\mathbb{P}_{cov|MBS} = \int_{\rho=0}^{\infty} \mathcal{L}_{I_v}(\epsilon_M T \rho^\alpha, 0) \mathcal{L}_{I_r}(\epsilon_M T \rho^\alpha, d_{th}) \mathcal{L}_{I_M}(\epsilon_M T \rho^\alpha, 0) 2\pi \lambda_a e^{-\lambda\pi\rho^2} \mathrm{d}\rho. \tag{4.28}$$

Like in the two inter-road communication schemes, we will now use the above results to obtain an overall expression for coverage probability in the next subsection.

4.3.4 Probability of Coverage: Final Expression

The final expression for coverage probability at a typical receiving node can be obtained by substituting the expressions obtained in Equations 4.27 and 4.28 into the overall coverage probability expression introduced in 4.3. Note that while the PDF of distance to the nearest MBS remains unchanged from the inter-road schemes, the vehicle being connected to now must lie on the same road as the receiver; so, the PDF of distance to transmitter when the receiver connects to the nearest vehicle is now $f_{d_r}(\rho) = 2\mu e^{-2\mu\rho}$, rather than the more complicated expression for $f_{d_v}(\rho)$ derived in Equation 3.3 and used for coverage probability calculations in the two previous schemes.

Theorem 3. *When only intra-road communication is allowed in the threshold distance-based scheme, the*

probability of coverage is given by:

$$\mathbb{P}_{cov} = \mathbb{P}_v \mathbb{P}_{cov|v} + \mathbb{P}_{MBS} \mathbb{P}_{cov|MBS}$$

$$= (1 - e^{-2\mu d_{th}}) \int_{\rho=0}^{d_{th}} \mathcal{L}_{I_v}(\epsilon_v T \rho^\alpha, 0) \mathcal{L}_{I_r}(\epsilon_v T \rho^\alpha, \rho) \mathcal{L}_{I_M}(\epsilon_v T \rho^\alpha, 0) 2\mu e^{-2\mu\rho} \mathrm{d}\rho$$

$$+ e^{-2\mu d_{th}} \int_{\rho=0}^{\infty} \mathcal{L}_{I_v}(\epsilon_M T \rho^\alpha, 0) \mathcal{L}_{I_r}(\epsilon_M T \rho^\alpha, d_{th}) \mathcal{L}_{I_M}(\epsilon_M T \rho^\alpha, 0) 2\pi \lambda_a e^{-\lambda\pi\rho^2} \mathrm{d}\rho. \qquad (4.29)$$

As mentioned before, the expressions for $\mathcal{L}_{I_v}, \mathcal{L}_{I_r}$ and $\mathcal{L}_{I_M}$ have already been derived in Equations 3.13, 3.15 and 3.16, respectively.

Chapter 5

Numerical Results and Discussion

In order to verify the accuracy of our analysis, we compare our theoretical results with simulation results in this Chapter. We chose to model a suburban area such as Blacksburg, Virginia. There are roughly 50 roads in its total perimeter of approximately 50 kilometres, i.e. $\lambda = 1km^{-1}$. Also, it has a relatively low vehicle density of about 1 vehicle per 100m. Since all vehicles may not have VANET connectivity, and not all vehicles are transmitting at the same instant of time, we have used a value of $\mu = 1km^{-1}$. Also, since current DSRC units transmit at around 0.5 W (24 dBm) and MBSs typically have a maximum transmit power of 50W, we have chosen $\epsilon_v = 100\epsilon_M$ for our simulations and analysis. In the following sections, we present the plots that compare the analytically obtained results with the simulated ones. *The analytical plots* (obtained by using the expressions derived in Chapters 3 and 4) *are presented using solid lines*, while the *the markers represent simulation results*.

5.1   Cellular Association Probabilities

The first parameter looked into is the cellular association probability, i.e., the probability that a receiving vehicle will choose to connect to its nearest MBS rather to a node in the vehicular network.
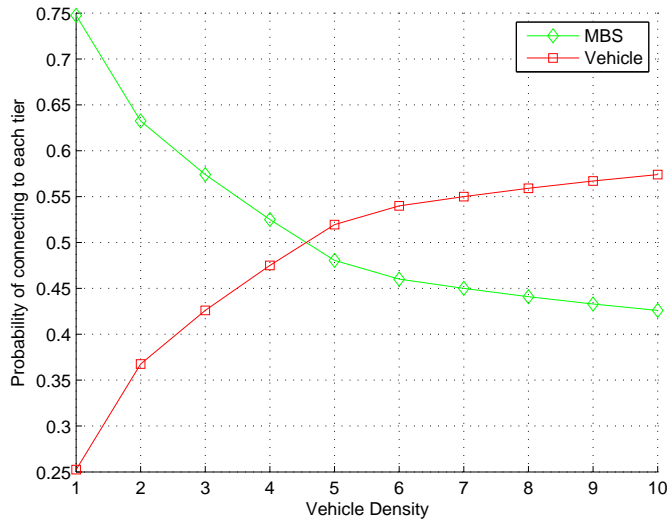
Figure 5.1: Vehicular and cellular association probabilities for the maximum average power-based scheme.

5.1.1 Maximum Power Based Scheme

In Lemmas 7 and 8, we had derived expressions for cellular and vehicular association probabilities, conditioned for a particular value of ρ. In order to obtain the overall association probabilities, we simply take these conditional probabilities ($\mathbb{P}_v(\rho)$ and $\mathbb{P}_{MBS}(\rho)$ respectively), and average them over the distribution of ρ. In other words, we obtain $\mathbb{P}_v$ and $\mathbb{P}_{MBS}$ as follows:

$$\mathbb{P}_v = \int_{\rho=0}^{\infty} \mathbb{P}_v(\rho) f_\rho d\rho \tag{5.1}$$

$$\mathbb{P}_{MBS} = \int_{\rho=0}^{\infty} \mathbb{P}_{MBS}(\rho) f_\rho d\rho \tag{5.2}$$

These expressions for $\mathbb{P}_v$ and $\mathbb{P}_{MBS}$ are plotted in Figure 5.1. It shows that using the current parameters (in which the vehicles transmit at only 1/100th the MBS power), the receiver chooses to connect to the cellular network very frequently, including situations when its own SIR was sufficiently high; this is not an ideal scenario because, as has been noted, it creates unnecessarily excessive load on the cellular network, loses much of the benefits of direct line-of-sight vehicular communications and makes the vehicular ad hoc network almost completely needless and redundant. Thus, in order to optimally reap the benefits of cellular-assisted VANETS, it is necessary to limit the probability of association to MBSs to some $k\%$ (the value of k depends on the cellular network and how much additional VANET traffic it is ready to handle).
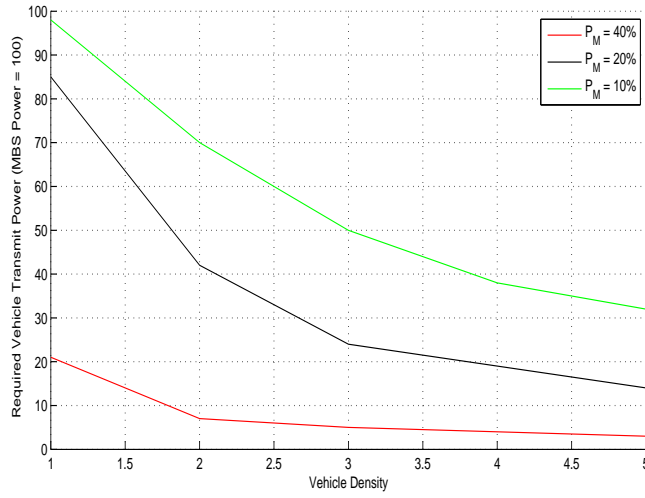
Figure 5.2: Required vehicle transmit power for different cellular association probabilities.

One way to ensure this is by having the vehicular nodes transmit at a higher power and thus reach out to a larger number of vehicles without having to switch to the cellular network. In order to test this hypothesis, we simulated the network for some different values of k, and plotted the minimum vehicular transmit power needed to limit the value of $\mathbb{P}_{MBS}$ to less than k. As we can see in Figure 5.2, increasing the transmit power of vehicles does reduce the cellular association probability of the vehicular network. For example, it is possible to limit cellular association probaility of a node to 10 % (at $\mu = \lambda = \lambda_a = 1$) by having the vehicles transmit at almost the same power as the cellular MBSs. In other words, one way to ensure that cellular-assisted VANETs do not produce excessive load on the cellular network, is to have higher vehicular transmit powers that can compare with the MBS transmit powers. There is, however, a potential flip-side to this solution: higher vehicle transmit powers could lead to more interference for the cellular network, thus deteriorating performance of the cellular network itself. Besides, significantly high transmit power for vehicles is not desirable from energy efficiency and even from health perspectives. This was one of the motivations behind defining threshold based inter-road and intra-road association schemes, which are discussed next.
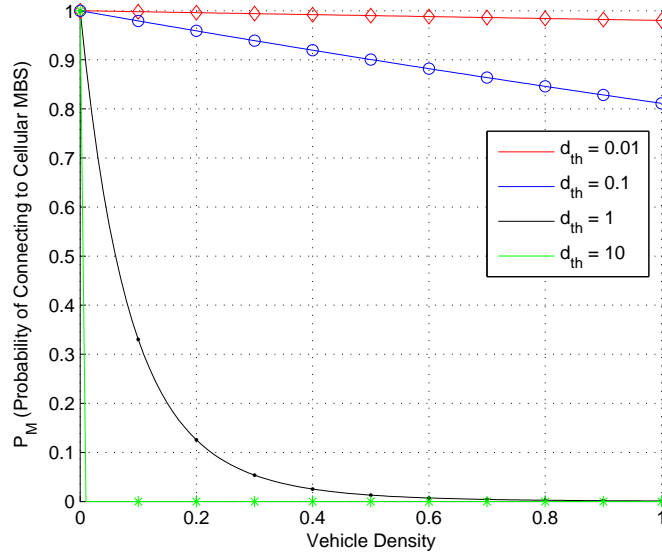
Figure 5.3: Probability of connecting to cellular network for threshold distance-based inter-road scheme. The theoretical result used here is presented in Lemma 13.

5.1.2 Threshold Distance Based Inter-Road Scheme

We now explore the cellular association probabilities ($\mathbb{P}_{MBS}$) for the theshold distance-based scheme in which inter-road communication is permitted. Figure 5.3 shows these association probabilities for four different threshold distances $(0.01, 0.1, 1$ and $10)$. From this plot, it can be seen that the probability of associating to the cellular network falls as the threshold distance increases. For example, at $d_{th} = 0.01$, this probability is almost 1, i.e., the receiver almost always connects to the nearest cellular MBS. A very high threshold distance (in comparison to average distance between vehicles) results in extremelylow values of $\mathbb{P}_{MBS}$. Both these situations are detrimental to network performance, thus, the ideal values of threshold distance lie in the same range as the average vehicle densities. For example, in the above plot, d_{th} values of 0.1 and 1 give a moderate value of cellular association probability, which would give a high network coverage without connecting too frequently to the cellular network. Also, note that $\mathbb{P}_{MBS}$ decreases when vehicle density μ increases. This is because of the fact that higher the vehicle density, more is the likelihood of there being at least one vehicle inside the threshold distance, which reduces the need to connect to the cellular network.
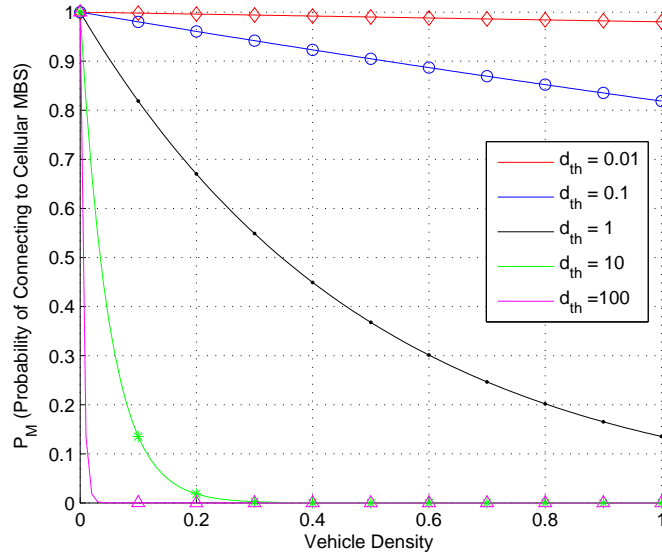
Figure 5.4: Probability of connecting to cellular network for threshold distance-based intra-road scheme. The theoretical result used here is presented in Lemma 15.

5.1.3 Threshold Distance Based Intra-Road Scheme

Figure 5.4 illustrates the cellular association probabilities for the intra-road scheme. Similar to the inter-road scheme, the cellular association probability in this case falls off when the threshold distance increases. Similarly, higher values of vehicle density μ also lead to lower values of cellular association probability.

5.1.4 Comparison

Figure 5.5 compares cellular association probabilities for the three schemes. Note that the receiver connects to the cellular MBSs most frequently in the maximum average power based scheme; this is because of the fact that the MBSs have a much higher transmit power as compared to the VANET nodes. In comparison, the threshold distance-based schemes have lower probabilities of associating with the cellular network. As has been noted, this is one of the major advantages of the threshold distance-based schemes; they connect more frequently to the VANET itself, thereby avoiding overloading cellular networks with additional vehicular traffic. Also, the receiver connects to the cellular network more frequently in the intra-road scheme as compared to the inter-road one. This higher value of $\mathbb{P}_{MBS}$ is one of the disadvantages of only allowing intra-
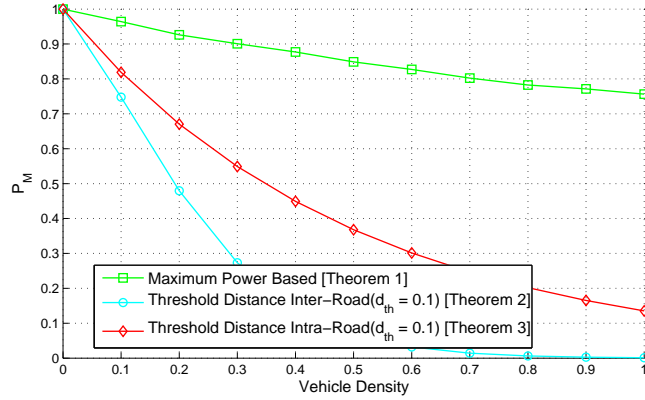
Figure 5.5: Probability of connecting to cellular network for different schemes.
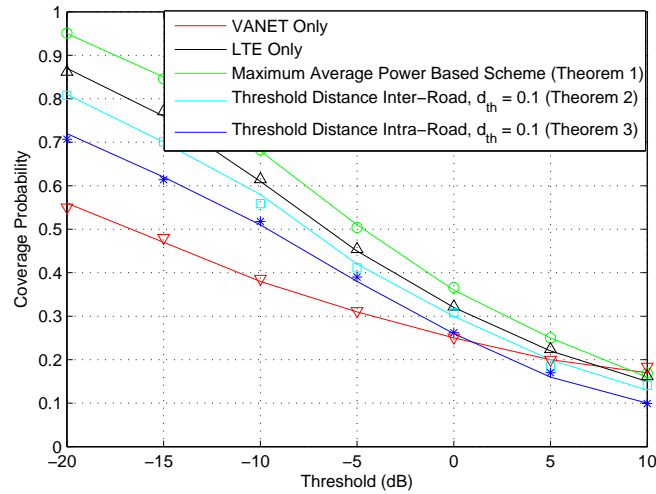

Figure 5.6: Coverage probability for various schemes studied in this thesis.

road communication, but it is compensated by the fact that it eliminates often unnecessary and redundant inter-road traffic from the vehicular network.

5.2 Probability of Coverage

Here, we compare the coverage in the three different schemes proposed in this thesis, with that in a non-assisted VANET and in a baseline cellular network. The results are presented in Figure 5.6.

As the plots reveal, the coverage in a VANET is improved by taking cellular assistance. Although the
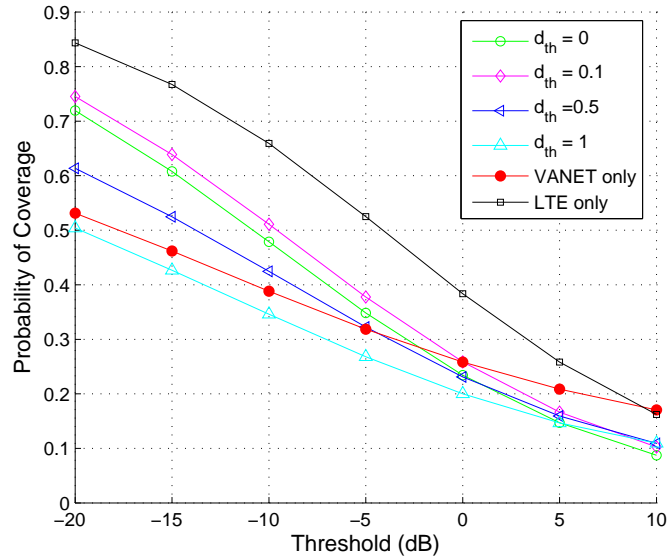
Figure 5.7: Coverage Probability of a node in intra-road threshold distance based scheme (Theorem 3).

cellular MBSs do generate additional interference, its effect is largely overshadowed by the coverage gain provided by these MBSs to the vehicles in case of loss of DSRC connectivity. Thus, the disadvantages of the stochastic and time-varying nature of a DSRC network can be overcome, to a great degree by the relatively more reliable cellular network. It is to be noted that coverage is best provided when the selection of transmitter is made on the basis of average power. In fact, this scheme even outperforms the coverage provided by a baseline cellular network. While using the threshold scheme provides slightly worse coverage, it is still much higher than a VANET that takes no support from the MBSs at all.

Now, we focus on one particular scheme: the threshold-distance based algorithm in which only intra-road communication is allowed. In Figure 5.7, we present coverage probability vs threshold SIR (T) for four different values of the threshold distance d_{th}, viz. $1, 0.5, 0.1$ and 0, where 0 implies that the typical node will always connect to the cellular network. These plots clearly reveal that the choice of threshold distance is critical to network performance. Lower threshold distances (e.g. $d_{th} = 0.1$) provide an improvement of coverage in comparison to a traditional VANET, while the network performs worse at higher threshold distances, since the VANET does not take support from the cellular network frequently enough, and the performance improvement achieved is overcome by the extra interference from the cellular network.

However, lower threshold distances also mean that the DSRC network will require cellular support more frequently, thus increasing cellular traffic and producing additional network load. So, reaping the benefits of this cellular-assisted VANET scheme will also entail producing more pressure on the existing cellular network (or on the RSU network, depending on the density of RSUs). Thus, there exists a tradeoff between reliability and additional cellular network load, controlled by the choice of threshold distance. The choice of an optimal threshold distance, that meets coverage reliability requirements and also minimizes additional cellular network traffic, is extremely vital for the improvement in performance gained by this scheme. This optimal distance will vary based on network requirements, density of vehicular traffic, spatial distribution of MBS's and several other network parameters, and the calculation of this optimal distance for different networks can be an interesting area of research that would reap immense benefits for the practical application of cellular-Assisted VANET in future vehicular networks.

Chapter 6

Conclusions and Future Work

In this thesis, we have used stochastic geometry to model and analyze several features of a vehicular ad hoc network, such as its interference, nearest neighbor distances and coverage. We have analyzed three different methodologies by which the coverage in such a network can be significantly improved by assistance from the existing cellular network in the case of loss of connectivity (or when the connectivity is better provided by the cellular network). While these MBSs do add extra interference, they also provide coverage to the vehicles which are too far away from the other nodes, and thus is capable of improving the probability of coverage of a typical node in the VANET. In fact, we have shown that if a receiver always connects to the network tier providing higher average power, it outperforms both the VANET and the cellular network in terms of coverage. Thus, using average power as a metric to swtich between cellular and VANET tiers can significantly improve VANET performance and improve their applicability for safety messaging purposes.

A comparitive study of the three proposed cellular-assistance methods has also been provided in this thesis; it shows that the average power-based scheme outperforms the two threshold distance-based schemes. It even provides better coverage than a baseline cellular network without any VANET interference. However, as has already been noted, the threshold distance based schemes can also provide reasonable acellularrnatives as they provide sufficiently good coverage while putting relatively less strain on already overloaded cellular networks. It can be concluded that the maximum power-based scheme is optimal where very high VANET performance is required, while VANETs in more latency-critical applications, or in scenarios where cellular

networks are already overloaded, threshold distance based schemes would likely be a preferred choice for the VANET operation. An interesting insight provided by this thesis is the dependence of coverage on the threshold distance. Lower threshold distances generally mean higher coverage, because of lower potential dominant interferers. However, low values of d_{th} could also mean higher cellular throughput demand, so deriving the optimal value of threshold distance for different applications could be a potential avenue for research and a boost for the application of cellular support in future VANETs.

From the stochastic geometry side, the Poisson Line Process based network model proposed in this thesis can be further improved by having two different kinds of transmitters in the network: a set of mobile vehicles transmitting at ϵ_v, and a set of road-side units transmitting at ϵ_R. This would give a three-tier network, rather than a two-tier network, and analyzing it could help understand the benefit provided by Road-Side Units vs. that provided by the cellular assistance. In addition, future models can incorporate more realistic fading models (such as Ricean fading) to provide a more accurate analysis of the vehicular network.

Chapter 7

Bibliography

[1] Y. Wang and F. Li, "Vehicular ad hoc networks," in *Guide to wireless ad hoc networks*. Springer, 2009, pp. 503–525.

[2] F. Ye, M. Adams, and S. Roy, "V2V wireless communication protocol for rear-end collision avoidance on highways," in *IEEE ICC Workshops*. IEEE, 2008, pp. 375–379.

[3] K. Dar, M. Bakhouya, J. Gaber, M. Wack, and P. Lorenz, "Wireless communication technologies for its applications [topics in automotive networking]," *IEEE Communications Magazine*, vol. 48, no. 5, pp. 156–162, 2010.

[4] L. Delgrossi and T. Zhang, "Dedicated short-range communications," *Vehicle Safety Communications: Protocols, Security, and Privacy*, pp. 44–51, 2009.

[5] J. Yin, T. ElBatt, G. Yeung, B. Ryu, S. Habermas, H. Krishnan, and T. Talty, "Performance evaluation of safety applications over DSRC vehicular ad hoc networks," in *Proceedings of the 1st ACM international workshop on Vehicular ad hoc networks*. ACM, 2004, pp. 1–9.

[6] M. Haenggi, *Stochastic geometry for wireless networks*. Cambridge University Press, 2012.

[7] J. F. C. Kingman, *Poisson processes*. Oxford university press, 1992, vol. 3.

[8] J. Santa, A. F. Gómez-Skarmeta, and M. Sánchez-Artigas, "Architecture and evaluation of a unified

V2V and V2I communication system based on cellular networks," *Computer Communications*, vol. 31, no. 12, pp. 2850–2861, 2008.

[9] Q. Xu, T. Mak, J. Ko, and R. Sengupta, "Vehicle-to-vehicle safety messaging in dsrc," in *Proceedings of the 1st ACM international workshop on Vehicular ad hoc networks*. ACM, 2004, pp. 19–28.

[10] S. Biswas, R. Tatchikou, and F. Dion, "Vehicle-to-vehicle wireless communication protocols for enhancing highway traffic safety," *IEEE Communications Magazine*, vol. 44, no. 1, pp. 74–82, 2006.

[11] H. H. Chang, S. J. Namkoong, Y.-I. Lee, and B.-J. Yoon, "Dynamic freeway path travel time prediction based on npr approach using dsrc data," in *Transportation Research Board 90th Annual Meeting*, no. 11-3063, 2011.

[12] A. Alhammad, F. Siewe, and A. H. Al-Bayatti, "An infostation-based context-aware on-street parking system," in *2012 International Conference on Computer Systems and Industrial Informatics (ICCSII)*. IEEE, 2012, pp. 1–6.

[13] P. Papadimitratos, A. La Fortelle, K. Evenssen, R. Brignolo, and S. Cosenza, "Vehicular communication systems: Enabling technologies, applications, and future outlook on intelligent transportation," *IEEE Communications Magazine*, vol. 47, no. 11, pp. 84–95, 2009.

[14] J. G. Andrews, "Seven ways that hetnets are a cellular paradigm shift," *IEEE Communications Magazine*, vol. 51, no. 3, pp. 136–144, 2013.

[15] Qualcomm, "LTE advanced: heterogeneous networks," white paper, Jan. 2011.

[16] J. G. Andrews, F. Baccelli, and R. K. Ganti, "A tractable approach to coverage and rate in cellular networks," *IEEE Transactions on Communications*, vol. 59, no. 11, pp. 3122–3134, 2011.

[17] D. Stoyan, W. S. Kendall, J. Mecke, and L. Ruschendorf, *Stochastic geometry and its applications*. Wiley New York, 1987, vol. 2.

[18] S. P. Weber and J. G. Andrews, *Transmission Capacity of Wireless Networks*. NOW: Foundations and Trends in Networking, 2012.

[19] M. Haenggi and R. K. Ganti, *Interference in Large Wireless Networks*. NOW: Foundations and Trends in Networking, 2008.

[20] H. S. Dhillon, R. K. Ganti, F. Baccelli, and J. G. Andrews, "Modeling and analysis of K-tier downlink heterogeneous cellular networks," *IEEE Journal on Selected Areas in Communications*, vol. 30, no. 3, pp. 550–560, 2012.

[21] H.-S. Jo, Y. J. Sang, P. Xia, and J. G. Andrews, "Heterogeneous cellular networks with flexible cell association: A comprehensive downlink SINR analysis," *IEEE Transactions on Wireless Communications,*, vol. 11, no. 10, pp. 3484–3495, 2012.

[22] S. Mukherjee, "Distribution of downlink SINR in heterogeneous cellular networks," *IEEE Journal on Selected Areas in Communications*, vol. 30, no. 3, pp. 575 – 585, Apr. 2012.

[23] H. S. Dhillon, R. K. Ganti, and J. G. Andrews, "Load-aware modeling and analysis of heterogeneous cellular networks," *IEEE Transactions on Wireless Communications*, vol. 12, no. 4, pp. 1666 – 1677, Apr. 2013.

[24] H. S. Dhillon and J. G. Andrews, "Downlink rate distribution in heterogeneous cellular networks under generalized cell selection," *IEEE Wireless Communications Letters*, vol. 3, no. 1, pp. 42–45, 2014.

[25] T. D. Novlan, H. S. Dhillon, and J. G. Andrews, "Analytical modeling of uplink cellular networks," *IEEE Transactions on Wireless Communications*, vol. 12, no. 6, pp. 2669 – 2679, Jun. 2013.

[26] M. Afshang, H. S. Dhillon, and P. H. J. Chong, "Modeling and performance analysis of clustered device-to-device networks," *arXiv preprint arXiv:1508.02668*, 2015.

[27] M. C. Erturk, S. Mukherjee, H. Ishii, and H. Arslan, "Distributions of transmit power and sinr in device-to-device networks," *IEEE Communications Letters*, vol. 17, no. 2, pp. 273–276, 2013.

[28] C.-h. Lee and M. Haenggi, "Interference and outage in poisson cognitive networks," *IEEE Transactions on Wireless Communications*, vol. 11, no. 4, pp. 1392–1401, 2012.

[29] H. ElSawy and E. Hossain, "Two-tier hetnets with cognitive femtocells: Downlink performance modeling and analysis in a multichannel environment," *IEEE Transactions on Mobile Computing*, vol. 13, no. 3, pp. 649–663, 2014.

[30] S. Bandyopadhyay and E. J. Coyle, "An energy efficient hierarchical clustering algorithm for wireless sensor networks," in *INFOCOM 2003. Twenty-Second Annual Joint Conference of the IEEE Computer and Communications.*, vol. 3. IEEE, 2003, pp. 1713–1723.

[31] M. Haenggi, J. G. Andrews, F. Baccelli, O. Dousse, and M. Franceschetti, "Stochastic geometry and random graphs for the analysis and design of wireless networks," *IEEE Journal on Selected Areas in Communications*, vol. 27, no. 7, pp. 1029–1046, 2009.

[32] H. ElSawy, E. Hossain, and M. Haenggi, "Stochastic geometry for modeling, analysis, and design of multi-tier and cognitive cellular wireless networks: A survey," *IEEE Communications Surveys & Tutorials*, vol. 15, no. 3, pp. 996–1019, 2013.

[33] F. Baccelli and B. Blaszczyszyn, *Stochastic Geometry and Wireless Networks, Volume I – Theory.* NOW: Foundations and Trends in Networking, 2009.

[34] ——, *Stochastic Geometry and Wireless Networks, Volume II – Applications.* NOW: Foundations and Trends in Networking, 2009.

[35] S. Busanelli, G. Ferrari, and R. Gruppini, "Performance analysis of broadcast protocols in vanets with poisson vehicle distribution," in *ITS Telecommunications (ITST), 2011 11th International Conference on.* IEEE, 2011, pp. 133–138.

[36] M. Mabiala, A. Busson, and V. Veque, "Inside vanet: hybrid network dimensioning and routing protocol comparison," in *65th IEEE Vehicular Technology Conference, 2007. VTC2007-Spring.* IEEE, 2007, pp. 227–232.

[37] R. Fujimoto, H. Wu, R. Guensler, and M. Hunter, "Evaluating vehicular networks: Analysis, simulation, and field experiments," in *Modeling and Simulation Tools for Emerging Telecommunication Networks.* Springer, 2006, pp. 289–308.

[38] R. Baeza-Yates, *Recent advances in applied probability*. Springer Science & Business Media, 2005.

[39] B. D. Ripley, *Stochastic simulation*. John Wiley & Sons, 2009, vol. 316.

[40] F. Morlot, "A population model based on a poisson line tessellation," in *WiOpt'12: Modeling and Optimization in Mobile, Ad Hoc, and Wireless Networks*, 2012, pp. 337–342.

[41] B. Blaszczyszyn and P. Muhlethaler, "Random linear multihop relaying in a general field of interferers using spatial aloha."

[42] W. Dershowitz and H. Einstein, "Characterizing rock joint geometry with joint system models," *Rock Mechanics and Rock Engineering*, vol. 21, no. 1, pp. 21–51, 1988.

[43] P. Madhusudhanan, J. G. Restrepo, Y. Liu, T. X. Brown, and K. R. Baker, "Downlink performance analysis for a generalized shotgun cellular system," *IEEE Transactions on Wireless Communications*, vol. 13, no. 12, pp. 6684–6696, 2014.